DOI: 10.24352/UB.OVGU-2017-066

TECHNISCHE MECHANIK, 35, 1, (2015), 1 – 30
submitted: February 5, 2014

Nonlinear In-Plane Stability of Heterogeneous Curved Beams under a Concentrated Radial Load at the Crown Point

L. Kiss, G. Szeidl

This paper is devoted to the stability problem of shallow curved beams provided that the beam is made of a heterogeneous material. It is assumed that (a) the radius of curvature is constant and (b) the Young's modulus and Poisson's number depend on the cross-sectional coordinates. We have the following objectives: (1) derivation of a model more accurate than those available in the literature, (2) determination of the critical load assuming that the beam is subjected to a constant radial dead load at the crown point, (3) comparison of the results obtained with solutions valid for homogeneous beams.

1 Introduction

It is well known that curved beams – shallow or deep – play an important role in various engineering structures including for instance roof structures, bridges or stiffeners in aerospace applications. Research on the mechanical behaviour of curved beams began in the 19th century – we remind the reader of a book by Bresse (1854) who found solutions to the horizontal and vertical displacements of a curved beam in terms of the axial force and the bending moment. Books by Love (1892 and 1893) and Love (1906) also present some solutions – see Chapter 21 for details. Hurlbrink (1907-1908) determined the critical pressure for a clamped beam if the centerline is inextensible. Extensibility of the beam is first taken into account in Chwalla and Kollbrunner (1938). The most important results achieved before the sixties are gathered in book Timoshenko and Gere (1961) – see Chapter 7 for details. Work on stability issues became more intensive in and after the sixties. An exact analysis is provided for a fixed shallow arch with rectangular cross-section in Schreyer and Masur (1965). The paper by DaDeppo and Schmidt (1969) is concerned with the determination of the critical load if a deep circular beam is subjected to a vertical force. It is shown by assuming an inextensible beam that quadratic terms should be taken into account in the analysis. These investigations are continued in paper DaDeppo and Schmidt (1974). Based on a continuous model, papers Dym (1973a) and Dym (1973b) are devoted to the buckling and post-buckling behaviour of pinned shallow arches under dead pressure. A summary of these results is published in the book Dym (1974, 2002). The thesis by Szeidl (1975) uses analytical methods to determine the Green function matrices of the extensible pinned-pinned and fixed-fixed circular beams and determines not only the natural frequencies but the critical loads as well if the beam is subjected to a radial dead load provided that the Fourier series of the load is known. Finite element solutions to the buckling problems are presented in various papers – see Noor and Peters (1981), Calboun and DaDeppo (1983), Elias and Chen (1988) and Wen and Suhendro (1991). It should be remarked that the higher order curvature terms are not included into the finite element models in the papers mentioned. The authors assume that the membrane strain is a quadratic function of the rotation field while the bending moment is a linear function of the generalized displacements. This fact was the reason for reconsidering the problem and for developing a more accurate finite element model by Pi and Trahair (1998). Analytical solutions to pinned-pinned and fixed-fixed shallow arches subjected to a vertical dead load at the crown point are provided in Bradford et al. (2002), Pi and Bradford (2008). Paper Pi et al. (2008) generalizes the results achieved in Bradford et al. (2002) for the case when the ends of the arch are rotationally restrained (are pinned and supported by torsional springs). Further investigations are devoted to this problem by Pi and Bradford (2012) under the assumption that the torsional springs at the two ends of the arch are different. The paper by R. A. M. Silveira and Goncalves (2013) should also be mentioned, since it develops a new numerical strategy for the nonlinear equilibrium and stability analysis of slender curved elements, such as arches, pipes and rings under unilateral constraints. It clarifies the influence of the foundation position (above or below the structure) and its stiffness on the nonlinear behavior and stability of curved structures. It is also worth mentioning the paper by Bateni and Eslami (2014). In this work the fundamental assumptions are the same as those in Bradford et al. (2002), except for one thing: the arch is made of a functionally graded material.

As regards the dynamical behaviour of curved beams it is worth citing survey papers Márkus and Nánási (1981), Chidamparam and Leissa (1993), Laura and Maurizi (1987), in which a number of references can be found. Papers by Nieh et al. (2003) and Huang et al. (2003) have dealt with the stability and vibration of circular and elliptic arches subjected to a constant and uniformly distributed vertical load. The extensibility of the centerline is taken into account in both papers. However shear deformation is considered for the circular beam only. The paper by Szabó and Királyfalvi (1999) is devoted, among others, to the issue how to take into account the fact in the stability investigations that the body considered (a circular ring) can have a rigid body motion. In-plane static and dynamic buckling of shallow pin-ended parabolic arches with a horizontal cable is investigated by Chen and Feng (2010). The authors provide approximate solutions to the lower and upper dynamic buckling loads under step loads.

The main objective of the present paper is threefold: (1) we would like to clarify what the governing equations are if the Young's modulus and Poisson's number depend on the cross-sectional coordinates (cross-sectional inhomogeneity). As regards the preliminaries in this respect we refer to papers Baksa and Ecsedi (2009); Ecsedi and Dluhi (2005) and Kiss (2012). (2) Assuming shallow curved beams but using a more accurate model than that presented in Bradford et al. (2002) and Pi et al. (2008) we would like to investigate what the changes are in the final results including the critical load. (3) In addition we shall examine whether the linear models can be used and if yes under what conditions.

The paper is organized in eight Sections and an Appendix. Section 2 presents the fundamental relations. The governing equations for the pre-buckling and post-buckling state are established in Section 3. Sections 4 and 5 provide formal solutions to pinned-pinned beams. Section 6 contains the most important computational results. The effect of heterogeneity on the buckling load is demonstrated via an example in Section 7. The last section is a conclusion in which a summary is given with an emphasis on the most important results.

2 Fundamental Relations

2.1 General Relations for the Pre-buckling State

At first we shall consider the fundamental relations for the curved beam in the coordinate system chosen for carrying out the necessary calculations and derivations. Figure 1 shows a part of the curved beam and the applied curvilinear coordinate system, which is attached to the so-called E-weighted centerline (or centerline for short) with constant initial radius ρ_o. The local base is formed by the unit vectors $\mathbf{e}_\xi$ (tangent to the centerline), $\mathbf{e}_\eta$ (perpendicular to the plane of the centerline) and $\mathbf{e}_\zeta$ (normal to the centerline). As has already been mentioned in the previous section, the beam has a cross-sectional inhomogeneity, i.e. the material parameters – the Young's modulus E and the Poison's number ν – are functions of the cross-sectional coordinates η and ζ (that is they are independent of ξ): $E(\eta,\zeta) = E(-\eta,\zeta)$, $\nu(\eta,\zeta) = \nu(-\eta,\zeta)$. Otherwise the material of the beam is isotropic. The cross-section of the curved beam is uniform and symmetric with respect to the coordinate plane (ξ,ζ). The centerline along which the coordinates $\xi = s$ are measured is assumed to remain in the coordinate plane (ξ,ζ). In Figure 1 the point in which the centerline intersects the cross-section is denoted by C. If the beam is heterogeneous this point does not coincide with the geometrical center S of the cross-section. The position of the point C can be obtained from the following condition

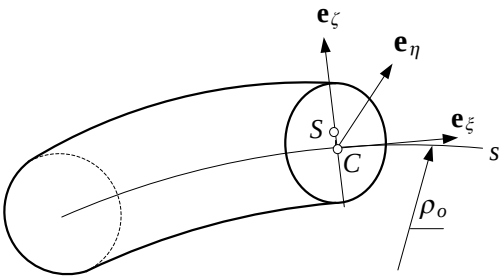

Figure 1: The coordinate system

$$Q_{e\eta} = \int_A E(\eta,\zeta)\,\zeta\,\mathrm{d}A = 0, \tag{1}$$

which means that the E-weighted first moment with respect to the axis η – this quantity is denoted by $Q_{e\eta}$ and is defined by the surface integral in the above equation – should vanish if the axis η passes through C. As regards the kinematic relations we assume that the displacement vector at an arbitrary point of the cross-section prior to buckling assumes the form

$$\mathbf{u} = \mathbf{u}_o + \psi_{o\eta}\zeta\mathbf{e}_\xi = w_o\mathbf{e}_\zeta + (u_o + \psi_{o\eta}\zeta)\mathbf{e}_\xi\ , \tag{2}$$

where $\mathbf{u}_o = u_o\mathbf{e}_\xi + w_o\mathbf{e}_\zeta$ is the displacement vector of the centerline and $\psi_{o\eta}$ is the rigid body rotation. As is well known the latter can be expressed in terms of the displacements as

$$\psi_{o\eta} = -\frac{1}{2}\left(\mathbf{u}\times\nabla\right)|_{\zeta=0}\cdot\mathbf{e}_\eta = \boldsymbol{\psi}|_{\zeta=0}\cdot\mathbf{e}_\eta = \frac{u_o}{\rho_o} - \frac{\mathrm{d}w_o}{\mathrm{d}s}\ . \tag{3}$$

Observe that the above relation is valid in the linear theory only. When determining the axial strain ε_ξ we have to use the Green-Lagrange strain tensor – Lagrangian description will be used throughout this paper – which consists of two parts:

$$\boldsymbol{E} = \boldsymbol{E}^L + \boldsymbol{E}^N\ ,\quad \boldsymbol{E}^L = \frac{1}{2}\left(\mathbf{u}\circ\nabla + \nabla\circ\mathbf{u}\right)\ ,\qquad \boldsymbol{E}^N = \frac{1}{2}\left(\nabla\circ\mathbf{u}\right)\cdot\left(\mathbf{u}\circ\nabla\right)\ . \tag{4}$$

Let

$$\boldsymbol{\Psi} = \frac{1}{2}\left(\mathbf{u}\circ\nabla - \nabla\circ\mathbf{u}\right)\ ,\quad \psi_\eta = \psi_\eta|_{\zeta=0} = \psi_{o\eta} = \mathbf{e}_\xi\cdot\boldsymbol{\Psi}\cdot\mathbf{e}_\eta\ ,\ \ \psi_\xi = \psi_{o\xi} = \psi_\zeta = \psi_{o\zeta} = 0 \tag{5}$$

be the tensor of small rotations – validity of relations $(5)_{2,3}$ follow from the kinematical hypotheses (2). We assume that the tensor of small rotations is dominant in comparison to the linear strains

$$\begin{aligned}\boldsymbol{E}^N = \frac{1}{2}\left(\nabla\circ\mathbf{u}\right)\cdot\left(\mathbf{u}\circ\nabla\right) = \frac{1}{2}\left(\boldsymbol{E}^L + \boldsymbol{\Psi}^T\right)\cdot\left(\boldsymbol{E}^L + \boldsymbol{\Psi}\right) = \\ = \frac{1}{2}\left(\boldsymbol{E}^L\cdot\boldsymbol{E}^L + \boldsymbol{\Psi}^T\cdot\boldsymbol{E}^L + \boldsymbol{E}^L\cdot\boldsymbol{\Psi} + \boldsymbol{\Psi}^T\cdot\boldsymbol{\Psi}\right) \approx \frac{1}{2}\boldsymbol{\Psi}^T\cdot\boldsymbol{\Psi} = \frac{1}{2}\boldsymbol{\Psi}\cdot\boldsymbol{\Psi}^T\ .\end{aligned} \tag{6}$$

Under this condition

$$\varepsilon_\xi = \mathbf{e}_\xi\cdot\frac{1}{2}\left(\mathbf{u}\circ\nabla + \nabla\circ\mathbf{u}\right)\cdot\mathbf{e}_\xi + \mathbf{e}_\xi\cdot\frac{1}{2}\left(\boldsymbol{\Psi}^T\cdot\boldsymbol{\Psi}\right)\cdot\mathbf{e}_\xi = \frac{1}{1+\frac{\zeta}{\rho_o}}\left(\varepsilon_{o\xi} + \zeta\kappa_o\right) + \frac{1}{2}\psi_{o\eta}^2 \tag{7}$$

is the axial strain, where

$$\varepsilon_{o\xi} = \frac{\mathrm{d}u_o}{\mathrm{d}s} + \frac{w_o}{\rho_o}\ ,\qquad \frac{\mathrm{d}\psi_{o\eta}}{\mathrm{d}s} = \kappa_o = \frac{1}{\rho_o}\frac{\mathrm{d}u_o}{\mathrm{d}s} - \frac{\mathrm{d}^2w_o}{\mathrm{d}s^2}\quad\text{and}\quad \varepsilon_m = \varepsilon_{o\xi} + \frac{1}{2}\psi_{o\eta}^2\ . \tag{8}$$

Here $\varepsilon_{o\xi}$ and ε_m are the linear and the nonlinear representations of the axial strain on the centerline, while κ_o is the curvature.

We shall further assume that the elements of the second Piola-Kirchhoff stress tensor satisfy the inequality $\sigma_\xi \gg \sigma_\eta, \sigma_\zeta$. Consequently $\sigma_\xi = E(\eta,\zeta)\varepsilon_\xi$ is the constitutive equation. With the knowledge of the stresses we can determine the inner forces in the initial configuration. For the sake of further considerations, we shall introduce three new quantities

$$A_{eR} = \int_A \frac{\rho_o}{\rho_o+\zeta}E(\eta,\zeta)\,\mathrm{d}A \simeq \int_A E(\eta,\zeta)\,\mathrm{d}A = A_e\ , \tag{9a}$$

$$I_{eR} = \int_A \frac{\rho_o}{\rho_o+\zeta}E(\eta,\zeta)\zeta^2\,\mathrm{d}A \simeq \int_A \zeta^2E(\eta,\zeta)\mathrm{d}A = I_{e\eta}\ , \tag{9b}$$

$$Q_{eR} = \int_A \frac{\rho_o}{\rho_o+\zeta}E(\eta,\zeta)\zeta\,\mathrm{d}A \simeq \frac{1}{\rho_o}\int_A \zeta^2E(\eta,\zeta)\,\mathrm{d}A = -\frac{I_{e\eta}}{\rho_o}\ . \tag{9c}$$

Here A_{eR} is referred to as the E-weighted reduced area, which is equal to the E-weighted area A_e with a good accuracy. The second quantity is denoted by I_{eR} and is named as the E-weighted reduced moment of inertia. Its value can be approximated by $I_{e\eta}$, which is the E-weighted moment of inertia with respect to the axis η. Finally Q_{eR} is the E-weighted reduced first moment.

Making use of Hooke's law, the kinematic equations (7), (8), and utilizing then the notations introduced by equations (9) we get the axial force as

$$\begin{aligned}N = \int_A E\varepsilon_\xi\,\mathrm{d}A = \underbrace{\int_A E\frac{1}{1+\frac{\zeta}{\rho_o}}\,\mathrm{d}A}_{A_{eR}\simeq A_e}\varepsilon_{o\xi} + \underbrace{\int_A E\frac{\zeta}{1+\frac{\zeta}{\rho_o}}\,\mathrm{d}A}_{Q_{eR}=-\frac{I_{e\eta}}{\rho_o}}\kappa_o + \underbrace{\int_A E\,\mathrm{d}A}_{A_e}\frac{1}{2}\psi_{o\eta}^2 = \\ = A_{eR}\varepsilon_{o\xi} + Q_{eR}\kappa_o + A_e\frac{1}{2}\psi_{o\eta}^2 \simeq A_e\underbrace{\left(\varepsilon_{o\xi} + \frac{1}{2}\psi_{o\eta}^2\right)}_{\varepsilon_m} - \frac{I_{e\eta}}{\rho_o}\kappa_o = A_e\varepsilon_m - \frac{I_{e\eta}}{\rho_o}\kappa_o\ .\end{aligned} \tag{10}$$

As regards the bending moment, a similar line of thought yields

$$M = \int_A E\varepsilon_\xi \zeta \,\mathrm{d}A = \int_A E\left(\frac{1}{1+\frac{\zeta}{\rho_o}}\left(\varepsilon_{o\xi}+\zeta\kappa_o\right)+\frac{1}{2}\psi_{o\eta}^2\right)\zeta\,\mathrm{d}A = -I_{e\eta}\left(\frac{\mathrm{d}^2 w_o}{\mathrm{d}s^2}+\frac{w_o}{\rho_o^2}\right) . \tag{11}$$

In what follows we shall assume that

$$\frac{A_e\rho_o^2}{I_{e\eta}} \gg 1 \quad \text{which is the same as} \quad \frac{A_e\rho_o^2}{I_{e\eta}} - 1 \approx \frac{A_e\rho_o^2}{I_{e\eta}} = m \, . \tag{12}$$

We shall also change derivatives with respect to s to derivatives with respect to φ by using the following equation

$$\frac{\mathrm{d}^n(\ldots)}{\mathrm{d}s^n} = \frac{1}{\rho_o^n}\frac{\mathrm{d}^n(\ldots)}{\mathrm{d}\varphi^n} = (\ldots)^{(n)} \;\; ; \quad n \in \mathbb{Z} \, . \tag{13}$$

This transformation is carried out everywhere without further remark. With the knowledge of the bending moment one can check – see equation (A.1) for details – that

$$N + \frac{M}{\rho_o} = A_e\varepsilon_m \, . \tag{14}$$

2.2 General Relations for the Post-buckling State

As regards the post-buckling equilibrium state let us now introduce a new notational convention. Quantities denoted by an asterisk belong to the post-buckling equilibrium state, while the change (increment) between the pre- and post-buckling equilibrium is denoted by a subscript $_b$. The change from the initial configuration to the pre-buckling state is not denoted by any symbol. Following this rule of decomposition – a similar line of thought as that applied in equations (3)-(8) – yields the increments in the kinematic relations. Presenting first formulae for the rotation field and the change of curvature we can write

$$\psi_{o\eta}^* = \psi_{o\eta} + \psi_{o\eta\, b} \, , \quad \psi_{o\eta\, b} = \frac{u_{ob}}{\rho_o} - \frac{\mathrm{d}w_{ob}}{\mathrm{d}s} \, , \quad \kappa_o^* = \kappa_o + \kappa_{o\, b} \, , \quad \kappa_{o\, b} = \frac{1}{\rho_o}\frac{\mathrm{d}u_{ob}}{\mathrm{d}s} - \frac{\mathrm{d}^2 w_{ob}}{\mathrm{d}s^2} \, . \tag{15}$$

Based on equation (8) we can use the previous decompositions to obtain the strain increment

$$\varepsilon_\xi^* = \frac{1}{1+\frac{\zeta}{\rho_o}}\left(\varepsilon_{o\xi}^* + \zeta\kappa_o^*\right) + \frac{1}{2}\left(\psi_{o\eta}^*\right)^2 = \varepsilon_\xi + \varepsilon_{\xi\, b}, \tag{16}$$

where

$$\varepsilon_{\xi\, b} = \frac{1}{1+\frac{\zeta}{\rho_o}}\left(\varepsilon_{o\xi\, b} + \zeta\kappa_{o\, b}\right) + \psi_{o\eta}\psi_{o\eta\, b} + \frac{1}{2}\psi_{o\eta\, b}^2 \, , \quad \varepsilon_{o\xi\, b} = \frac{\mathrm{d}u_{ob}}{\mathrm{d}s} + \frac{w_{ob}}{\rho_o} \, , \tag{17a}$$

$$\varepsilon_{mb} = \varepsilon_{\xi\, b}|_{\zeta=0} = \varepsilon_{o\xi\, b} + \psi_{o\eta}\psi_{o\eta\, b} + \frac{1}{2}\psi_{o\eta\, b}^2 \, . \tag{17b}$$

Observe that the rotational term quadratic in the increment has been neglected since we assume the applicability of the inequality $\frac{1}{2}\psi_{o\eta\, b}^2 \ll \psi_{o\eta}\psi_{o\eta\, b}$.

After having set up the kinematical relations we shall proceed with the derivation of those formulae, which provide the inner forces. Recalling equation (10) valid for the pre-buckling axial force and making use of the kinematic equations $(15)_1$, $(15)_3$, $(17a)_1$ and (17b) we can write

$$N^* = \int_A E\varepsilon_\xi^* \,\mathrm{d}A = A_{eR}\varepsilon_{o\xi}^* + Q_{eR}\kappa_o^* + A_e\frac{1}{2}\left(\psi_{o\eta}^*\right)^2 = A_e\varepsilon_m - \frac{I_{e\eta}}{\rho_o}\kappa_o + A_e\varepsilon_{m\, b} - \frac{I_{e\eta}}{\rho_o}\kappa_{ob} = N + N_b \, . \tag{18}$$

The increment in the axial force N_b can be manipulated into its final form if we utilize (12); $(15)_4$; $(17a)_2$ and (17b) – see equation (A.2) for details –

$$N_b = \frac{I_{e\eta}}{\rho_o^2} m\varepsilon_{mb} + \frac{I_{e\eta}}{\rho_o^3}\left(w_{ob}^{(2)} + w_{ob}\right) \, . \tag{19}$$

Due to the presence of the term ε_{mb} this result is nonlinear. It can be checked with ease by recalling (11) that

$$M^* = -I_{e\eta}\left(\frac{\mathrm{d}^2 w_o^*}{\mathrm{d}s^2} + \frac{w_o^*}{\rho_o^2}\right) = -I_{e\eta}\left(\frac{\mathrm{d}^2 w_o}{\mathrm{d}s^2} + \frac{w_o}{\rho_o^2}\right) \underbrace{-I_{e\eta}\left(\frac{\mathrm{d}^2 w_{ob}}{\mathrm{d}s^2} + \frac{w_{ob}}{\rho_o^2}\right)}_{M_b} = M + M_b \tag{20}$$

is the bending moment. With regard to equations (13) and (20) it follows from (19) that

$$N_b = \frac{I_{e\eta}}{\rho_o^2}\left(\frac{A_e\rho_o^2}{I_{e\eta}} - 1\right)\varepsilon_{mb} - \frac{M_b}{\rho_o} \approx A_e\varepsilon_{mb} - \frac{M_b}{\rho_o} \quad \text{from where} \quad N_b + \frac{M_b}{\rho_o} = A_e\varepsilon_{mb}\,. \tag{21}$$

3 Governing Equations

3.1 Equilibrium Conditions for the Pre-buckling State

Figure 2 shows the centerline of the beam considered in the initial configuration (continuous line) as well as in the pre-buckling equilibrium state (dashed line) assuming symmetrical conditions. The beam has rotationally restrained pins at both ends with a torsional spring constant $(k_{\gamma\ell})[k_{\gamma r}]$ at the (left) [right] end. The pre-buckling state is symmetric if the equality $k_{\gamma\ell} = k_{\gamma r} = k_\gamma$ holds - this is an assumption. The loading consists of the distributed forces $\mathbf{f} = f_t\mathbf{e}_\xi + f_n\mathbf{e}_\zeta$ and a concentrated force P_ζ – the former is exerted at the crown point. The central angle of the beam is 2ϑ. For the pre-buckling state the principle of virtual work can be written as

$$\int_V \sigma_\xi\delta\varepsilon_\xi\,\mathrm{d}V = -P_\zeta\;\delta w_o|_{s=0} - k_{\gamma\ell}\psi_{o\eta}\delta\psi_{o\eta}|_{s(-\vartheta)} - k_{\gamma r}\psi_{o\eta}\delta\psi_{o\eta}|_{s(\vartheta)} + \int_{\mathcal{L}}(f_n\delta w_o + f_t\delta u_o)\;\mathrm{d}s\,. \tag{22}$$

The principle of virtual work can be manipulated in a form which makes it possible to find the equilibrium conditions, the dynamic boundary conditions as well as the continuity and discontinuity conditions at the crown point. Details are presented in Section A.1.2. With a regard to the arbitrariness of the virtual quantities δu_o, δw_o and $\delta\psi_{o\eta}$ in equation (A.5) we have the following equilibrium equations

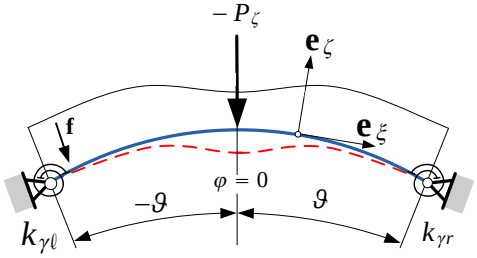

Figure 2: A curved beam

$$\frac{\mathrm{d}N}{\mathrm{d}s} + \frac{1}{\rho_o}\left[\frac{\mathrm{d}M}{\mathrm{d}s} - \left(N + \frac{M}{\rho_o}\right)\psi_{o\eta}\right] + f_t = 0\,, \qquad \frac{\mathrm{d}}{\mathrm{d}s}\left[\frac{\mathrm{d}M}{\mathrm{d}s} - \left(N + \frac{M}{\rho_o}\right)\psi_{o\eta}\right] - \frac{N}{\rho_o} + f_n = 0\,. \tag{23}$$

It also follows from (A.5) that boundary conditions can be imposed on the following quantities

$$N|_{s(\pm\vartheta)} \quad \text{or} \quad u_o|_{s(\pm\vartheta)}\,, \tag{24a}$$

$$\left[\frac{\mathrm{d}M}{\mathrm{d}s} - \left(N + \frac{M}{\rho_o}\right)\psi_{o\eta}\right]\Big|_{s(\pm\vartheta)} \quad \text{or} \quad w_o|_{s(\pm\vartheta)}\,, \tag{24b}$$

$$(M \pm k_\gamma\psi_{o\eta})|_{s(\pm\vartheta)} \quad \text{or} \quad \psi_{o\eta}|_{s(\pm\vartheta)}\,. \tag{24c}$$

The discontinuity condition

$$\left[\frac{\mathrm{d}M}{\mathrm{d}s} - \left(N + \frac{M}{\rho_o}\right)\psi_{o\eta}\right]\Big|_{s=+0} - \left[\frac{\mathrm{d}M}{\mathrm{d}s} - \left(N + \frac{M}{\rho_o}\right)\psi_{o\eta}\right]\Big|_{s=-0} - P_\zeta = 0 \tag{25}$$

for the shear force should also be satisfied.

3.2 Equilibrium Equations in Terms of the Displacements

In the sequel we focus on the problem for which there is only a concentrated dead load P_ζ exerted at the crown of the beam, i.e., the distributed force components f_n and f_t are equal to zero. It is our aim to express the equilibrium

equations in terms of the displacements. As for $(23)_1$ let us first substitute relation (14) for the inner forces. We get

$$\frac{\mathrm{d}}{\mathrm{d}s}\left(A_e\varepsilon_m\right) - \frac{1}{\rho_o}\left(A_e\varepsilon_m\psi_{o\eta}\right) = 0\,. \tag{26}$$

It can be assumed with a good accuracy that the product $\varepsilon_m\psi_{o\eta}$ – being quadratic in the displacements, see (3) and (8) – can be neglected when it is compared to the first term. Accordingly, the pre-buckling equilibrium can be expressed in the following form

$$\frac{\mathrm{d}\varepsilon_m}{\mathrm{d}s} \simeq \frac{\mathrm{d}\varepsilon_{o\xi}}{\mathrm{d}s} = 0 \quad \rightarrow \quad \varepsilon_m \simeq \varepsilon_{o\xi} = \text{constant}\,. \tag{27}$$

Hence (depending on which theory is applied) the nonlinear/linear strain on the centerline is constant.

Some manipulations should be made on equation $(23)_2$. These are detailed in Section A.1.4. Here the final form on which the stability investigations will be based is presented only

$$W_o^{(4)} + \left(\chi^2+1\right)W_o^{(2)} + \chi^2 W_o = \chi^2 - 1\,, \qquad \chi^2 = 1 - m\varepsilon_m. \tag{28}$$

Observe that we have introduced a new notation $W_o = w_o/\rho_o$, which is referred to as the dimensionless displacement. For the sake of brevity we have also introduced a new variable χ.

Equation (28) can now be compared with what Bradford et al. have used in their series of articles published recently on stability problems of shallow arches – e.g. Bradford et al. (2002); Pi et al. (2008). This equation is of the form

$$W_o^{(4)} + (\chi^2 - 1)W_o^{(2)} = \chi^2 - 1 \tag{29}$$

– compare it with equation (14) in Bradford et al. (2002). The effects of our keeping the additional terms will be evaluated later in Section 6. However we hope that more accurate results can be obtained by utilizing equation (28) in the stability investigations of shallow curved beams.

3.3 Equilibrium Conditions after the Loss of Stability

The principle of virtual work for the buckled equilibrium configuration assumes the form

$$\int_V \sigma_\xi^*\delta\varepsilon_\xi^*\,\mathrm{d}V = -P_\zeta^*\,\delta w_o^*|_{s=0} + P_\xi^*\,\delta u_o^*|_{s=0} - \mathfrak{m}\ddot{w}_o^*\delta w_o^*|_{s=0} - \mathfrak{m}\ddot{u}_o^*\delta u_o^*|_{s=0} - \\ - k_{\gamma\,\ell}\psi_{o\eta}^*\delta\psi_{o\eta}^*\big|_{s(-\vartheta)} - k_{\gamma\,r}\psi_{o\eta}^*\delta\psi_{o\eta}^*\big|_{s(\vartheta)} + \int_{\mathcal{L}}\left(f_n^*\delta w_o^* + f_t^*\delta u_o^*\right)\mathrm{d}s, \tag{30}$$

where $\ddot{w}_o^*$ and $\ddot{u}_o^*$ are the second time derivatives of the two displacements.

Here it is assumed that the stability loss is a dynamical process characterized by a mass $\mathfrak{m}$ placed at the crown point of the beam (where the concentrated force acts). In other words the effect of the mass distribution on the centerline is modelled by the concentrated mass at the crown point. We have not made any restriction concerning the behaviour of the load, that is, it can either be a dead one, or a follower one. However we shall assume a dead load later. Apart from these changes (30) coincides formally with (22).

After some manipulations, which are detailed in Section A.1.3, it can be shown that the arbitrariness of the virtual quantities yield the equations

$$\frac{\mathrm{d}N_b}{\mathrm{d}s} + \frac{1}{\rho_o}\frac{\mathrm{d}M_b}{\mathrm{d}s} - \frac{1}{\rho_o}\left(N + \frac{M}{\rho_o}\right)\psi_{o\eta\,b} - \frac{1}{\rho_o}\left(N_b + \frac{M_b}{\rho_o}\right)\psi_{o\eta\,b} + f_{tb} = 0\,, \tag{31a}$$

$$\frac{\mathrm{d}^2M_b}{\mathrm{d}s^2} - \frac{N_b}{\rho_o} - \frac{\mathrm{d}}{\mathrm{d}s}\left[\left(N + N_b + \frac{M+M_b}{\rho_o}\right)\psi_{o\eta\,b} + \left(N_b + \frac{M_b}{\rho_o}\right)\psi_{o\eta}\right] + f_{nb} = 0, \tag{31b}$$

which describe the post-buckling equilibrium. Moreover

$$\left[\frac{\mathrm{d}M_b}{\mathrm{d}s} - \left(N + N_b + \frac{M+M_b}{\rho_o}\right)\psi_{o\eta\,b} - \left(N_b + \frac{M_b}{\rho_o}\right)\psi_{o\eta}\right]\Bigg|_{s=-0} - \tag{32a}$$

$$- \left[\frac{\mathrm{d}M_b}{\mathrm{d}s} - \left(N + N_b + \frac{M+M_b}{\rho_o}\right)\psi_{o\eta\,b} - \left(N_b + \frac{M_b}{\rho_o}\right)\psi_{o\eta}\right]\Bigg|_{s=+0} + \mathfrak{m}\,\frac{\mathrm{d}^2w_{ob}}{\mathrm{d}t^2}\Bigg|_{s=0} = 0\,,$$

$$N_b|_{s=-0} - N_b|_{s=+0} + P_{\xi\, b} + \mathfrak{m}\, \frac{\mathrm{d}^2 u_{ob}}{\mathrm{d}t^2}\bigg|_{s=0} = 0 \tag{32b}$$

are the discontinuity conditions at the crown point. It follows from (A.12) that boundary conditions can be imposed on the following quantities

$$N_b|_{s(\pm\vartheta)} \qquad \text{or} \qquad u_{ob}|_{s(\pm\vartheta)}\ , \tag{33a}$$

$$\left[\frac{\mathrm{d}M_b}{\mathrm{d}s} - \left(N + N_b + \frac{M + M_b}{\rho_o}\right)\psi_{o\eta\, b} - \left(N_b + \frac{M_b}{\rho_o}\right)\psi_{o\eta}\right]\bigg|_{s(\pm\vartheta)} \qquad \text{or} \qquad w_{ob}|_{s(\pm\vartheta)}\ , \tag{33b}$$

$$(M_b \pm k_\gamma \psi_{o\eta\, b})|_{s(\pm\vartheta)} \qquad \text{or} \qquad \psi_{o\eta\, b}|_{s(\pm\vartheta)}\ . \tag{33c}$$

Observe that we have kept the nonlinear terms in the boundary conditions as well.

3.4 Post-buckling Equilibrium Equations in Terms of the Displacements

Assume now – as in Subsection 3.2 – that there is only a dead load, the force P_ζ exerted at the crown of the beam, and there is no concentrated mass $\mathfrak{m}$ at its point of application: $f_{nb} = f_{tb} = P_{\xi\, b} = P_{\zeta\, b} = \mathfrak{m} = 0$. Observe that the structure of equilibrium equation (31a) is very similar to that of $(23)_1$. The exception is the fourth term in (31a) as it does not appear in the pre-buckling relation. However it can be neglected since that product is quadratic in the increments. Therefore repeating the line of thought presented in Subsection 3.2 now for the increments, it follows that (both for the nonlinear and for the linear models) the change in the axial strain is constant:

$$\frac{\mathrm{d}}{\mathrm{d}s}\left(A_e \varepsilon_{mb}\right) - \underbrace{\frac{1}{\rho_o}\left(A_e \varepsilon_m \psi_{o\eta b}\right)}_{\text{it can also be neglected}} = 0 \quad \Rightarrow \quad \frac{\mathrm{d}\varepsilon_{m\, b}}{\mathrm{d}s} \simeq \frac{\mathrm{d}\varepsilon_{o\xi\, b}}{\mathrm{d}s} = 0 \quad \rightarrow \quad \varepsilon_{m\, b} \simeq \varepsilon_{o\xi\, b} = \text{constant}\ . \tag{34}$$

Section A.1.5 is devoted to the detailed manipulations on equilibrium equation (31b). The resulting relation of these follows from (A.20)

$$W_{ob}^{(4)} + (\chi^2 + 1) W_{ob}^{(2)} + \chi^2 W_{ob} = m\varepsilon_{mb}\left[1 - \left(W_o^{(2)} + W_o\right)\right]\ , \tag{35}$$

where $W_{ob} = w_{ob}/\rho_o$ is the dimensionless displacement increment.

If we recall equation (39) in Bradford et al. (2002) for the stability investigation of shallow circular arches then we get with our notations

$$W_{ob}^{(4)} + (\chi^2 - 1) W_{ob}^{(2)} = m\varepsilon_{mb}\left(1 - W_o^{(2)}\right)\ . \tag{36}$$

The differences are easily noticeable if we compare (36) with (35).

4 Solution to the Pre-buckling State

4.1 General Solution

The differential equations that describe the equilibrium state of the beam prior to buckling are gathered in Section 3.2 – we refer back to equations (27) and (28). The general solution satisfying equation (28) set up for the dimensionless normal displacement is sought separately on the left ($W_{o\,\ell}$) and on the right ($W_{o\,r}$) half beam (due to the discontinuity in the shear force) in the forms

$$W_{o\,r} = \frac{\chi^2 - 1}{\chi^2} + A_1 \cos\varphi + A_2 \sin\varphi - \frac{A_3}{\chi^2}\cos\chi\varphi - \frac{A_4}{\chi^2}\sin\chi\varphi\ , \tag{37a}$$

$$W_{o\,\ell} = \frac{\chi^2 - 1}{\chi^2} + B_1 \cos\varphi + B_2 \sin\varphi - \frac{B_3}{\chi^2}\cos\chi\varphi - \frac{B_4}{\chi^2}\sin\chi\varphi\ . \tag{37b}$$

Here A_i and B_i $(i = 1, \ldots, 4)$ are undetermined integration constants. These can be determined with the knowledge of the boundary conditions.

4.2 Pinned-pinned Beam

Since the geometry, the loading, and the supports ($k_{\gamma\, r} = k_{\gamma\, \ell} = 0$) are all symmetric it is obvious that the radial displacement is an even function of the angle coordinate: $W_o(\varphi) = W_o(-\varphi)$. Therefore it is sufficient to consider, say, the right half of the beam. As regards the boundary conditions, the tangential displacement and the rotation are zero, and there is a jump in the shear force with magnitude $P_\zeta/2$ if $\varphi = 0$. In addition the displacement and the bending moment are also zero at the right end of the beam. The corresponding boundary conditions are gathered in Table 1.

Table 1: Boundary conditions for the pinned beam

Boundary conditions		Boundary conditions in terms of $W_{o\,r}$	
Crown point	Right end	Crown point	Right end
$\psi_{o\eta}\big\vert_{\varphi=+0} = 0$	$W_{o\,r}\big\vert_{\varphi=\vartheta} = 0$	$W_{o\,r}^{(1)}\Big\vert_{\varphi=+0} = 0$	$W_{o\,r}\big\vert_{\varphi=\vartheta} = 0$
$\left[-\frac{\mathrm{d}M}{\mathrm{d}s} + \frac{P_\zeta}{2}\right]_{\varphi=+0} = 0$	$M\big\vert_{\varphi=\vartheta} = 0$	$I_{e\eta} W_{o\,r}^{(3)}\Big\vert_{\varphi=+0} = \frac{P_\zeta}{2}$	$W_{o\,r}^{(2)}\Big\vert_{\varphi=\vartheta} = 0$

After substituting the solution $W_{o\,r}$ into the boundary conditions we get a system of linear equations

$$\begin{bmatrix} 0 & \chi & 0 & -1 \\ 0 & 0 & 0 & 1 \\ \cos\vartheta & \sin\vartheta & -\frac{1}{\chi^2}\cos\chi\vartheta & -\frac{1}{\chi^2}\sin\chi\vartheta \\ -\cos\vartheta & -\sin\vartheta & \cos\chi\vartheta & \sin\chi\vartheta \end{bmatrix} \begin{bmatrix} A_1 \\ A_2 \\ A_3 \\ A_4 \end{bmatrix} = \begin{bmatrix} 0 \\ \frac{\chi}{\chi^2-1}\frac{\mathcal{P}}{\vartheta} \\ -\frac{\chi^2-1}{\chi^2} \\ 0 \end{bmatrix}, \quad \mathcal{P} = -\frac{P_\zeta}{2}\frac{\rho_o^2\vartheta}{I_{e\eta}} \tag{38}$$

in which $\mathcal{P}$ is a dimensionless force. Observe that the solutions

$$\begin{aligned} A_1 &= -\frac{1}{\cos\vartheta} - \frac{\tan\vartheta}{\chi^2-1}\frac{\mathcal{P}}{\vartheta} = A_{11} + A_{12}\frac{\mathcal{P}}{\vartheta}\,, \qquad A_2 = \frac{1}{\chi^2-1}\frac{\mathcal{P}}{\vartheta} = A_{22}\frac{\mathcal{P}}{\vartheta}\,, \\ A_3 &= -\frac{1}{\cos\chi\vartheta} - \frac{\chi\tan\chi\vartheta}{\chi^2-1}\frac{\mathcal{P}}{\vartheta} = A_{31} + A_{32}\frac{\mathcal{P}}{\vartheta}\,, \quad A_4 = \frac{\chi}{\chi^2-1}\frac{\mathcal{P}}{\vartheta} = A_{42}\frac{\mathcal{P}}{\vartheta} \end{aligned} \tag{39}$$

are decomposed into the sum of two parts depending on whether these are in relation with the loading (A_{i2}) or not (A_{i1}). Now the closed form solution for the full beam can be constructed if we introduce the function

$$H(\varphi) = \begin{cases} -1 & \varphi < 0 \\ 1 & \varphi > 0 \end{cases} \tag{40}$$

by the use of which

$$W_o = \frac{\chi^2-1}{\chi^2} + A_{11}\cos\varphi - \frac{A_{31}}{\chi^2}\cos\chi\varphi + \left(A_{12}\cos\varphi + A_{22}H\sin\varphi - \frac{A_{32}}{\chi^2}\cos\chi\varphi - \frac{A_{42}}{\chi^2}H\sin\chi\varphi\right)\frac{\mathcal{P}}{\vartheta} \tag{41}$$

is the radial displacement. With this in hand

$$\begin{aligned} \psi_{o\eta} = U_o - W_o^{(1)} \simeq -W_o^{(1)} &= A_{11}\sin\varphi - \frac{A_{31}}{\chi}\sin\chi\varphi + \\ &+ \left(A_{12}\sin\varphi - A_{22}H\cos\varphi - \frac{A_{32}}{\chi}\sin\chi\varphi + \frac{A_{42}}{\chi}H\cos\chi\varphi\right)\frac{\mathcal{P}}{\vartheta} = \\ &= D_{11}\sin\varphi + D_{31}\sin\chi\varphi + (D_{12}\sin\varphi + D_{22}\cos\varphi + D_{32}\sin\chi\varphi + D_{42}\cos\chi\varphi)\frac{\mathcal{P}}{\vartheta} \end{aligned} \tag{42a}$$

is the rotation field. Here we have assumed and in the sequel we shall assume that the tangential displacement has a negligible effect on the rotation field. The constants D_{ij} $i, j \in [1, 2, 3, 4]$ are defined by

$$D_{11} = A_{11}\,, \quad D_{12} = A_{12}\,, \quad D_{22} = -A_{22}H\,, \quad D_{31} = -\frac{A_{31}}{\chi}\,, \quad D_{32} = -\frac{A_{32}}{\chi}\,, \quad D_{42} = \frac{A_{42}H}{\chi}\,. \tag{42b}$$

It follows from the equilibrium equation (27) that the axial strain $(8)_1$ is constant on the centerline. Let us calculate the mathematical average of this quantity. We have

$$\varepsilon_{o\,\xi} \;=\; \frac{1}{\vartheta}\int_0^{\vartheta}\varepsilon_{o\,\xi}(\varphi)\mathrm{d}\varphi \;=\; \frac{1}{\vartheta}\int_0^{\vartheta}\left(U_{o\,r}^{(1)}+W_{o\,r}\right)\mathrm{d}\varphi \;=\; \frac{1}{\vartheta}\int_0^{\vartheta}W_{o\,r}\mathrm{d}\varphi \;=\; I_{ow}\;+\;I_{1w}\frac{\mathcal{P}}{\vartheta}\quad . \tag{43}$$

The above equation is linear in $\mathcal{P}$ and is nonlinear in $\varepsilon_{o\,\xi}$ – see the definition of χ under $(28)_2$ – now $\varepsilon_{o\,\xi}=\varepsilon_m$. We remark that the integrals I_{ow} and I_{1w} are presented in a closed form in Section A.1.6. Equation (43) can be rearranged as

$$I_{1w}\frac{\mathcal{P}}{\vartheta}+I_{ow}-\varepsilon_{o\xi}=0\;. \tag{44}$$

If we assume that the axial strain is given by $(8)_3$ then the procedure leading to (43) results in

$$\varepsilon_m \;=\; \frac{1}{\vartheta}\int_0^{\vartheta}\varepsilon_m(\varphi)\mathrm{d}\varphi \;=\; \frac{1}{\vartheta}\int_0^{\vartheta}\left(\varepsilon_{o\xi}+\frac{1}{2}\psi_{o\eta}^2\right)\mathrm{d}\varphi \;=\; I_{ow}+I_{1w}\frac{\mathcal{P}}{\vartheta}+I_{o\psi}+I_{1\psi}\frac{\mathcal{P}}{\vartheta}+I_{2\psi}\left(\frac{\mathcal{P}}{\vartheta}\right)^2 \tag{45}$$

or

$$I_{2\psi}\left(\frac{\mathcal{P}}{\vartheta}\right)^2+\left(I_{1w}+I_{1\psi}\right)\frac{\mathcal{P}}{\vartheta}+\left(I_{ow}+I_{o\psi}-\varepsilon_m\right)=0\;. \tag{46}$$

This is a more accurate relationship between the load and the axial strain. The new integrals $I_{o\psi}$, $I_{1\,\psi}$ and $I_{2\psi}$ are again gathered in closed forms in Section A.1.6.

At the same time we remark that the integrations can be carried out numerically by using the subroutine `DQDAG` from the IMSL Library under the Fortran90 programming language. We have come to the conclusion that the accuracy of this routine is more than sufficient for this problem with its maximum error being less than 10^{-7}.

5 Solutions to the Post-buckling State

5.1 General Solutions

After substituting the pre-buckling solution (41) into the right side of equation (35) we get

$$W_{ob}^{(4)}+(1+\chi^2)W_{ob}^{(2)}+\chi^2W_{ob}=-m\varepsilon_{mb}\frac{1-\chi^2}{\chi^2}\left(\frac{1}{1-\chi^2}+A_3\cos\chi\varphi+A_4\sin\chi\varphi\right)\;. \tag{47}$$

Recalling that the post buckling axial strain on the E-weighted centerline is constant and can be calculated as

$$\varepsilon_{mb}\simeq\frac{1}{2\vartheta}\int_{-\vartheta}^{\vartheta}\left(U_{ob}^{(1)}+W_{ob}+\psi_{o\eta\,b}\psi_{o\eta}\right)\mathrm{d}\varphi=\frac{1}{2\vartheta}\int_{-\vartheta}^{\vartheta}\left(U_{ob}^{(1)}+W_{ob}+\left(U_{ob}-W_{ob}^{(1)}\right)\left(U_o-W_o^{(1)}\right)\right)\mathrm{d}\varphi\approx$$
$$\approx\frac{1}{2\vartheta}\int_{-\vartheta}^{\vartheta}\left(U_{ob}^{(1)}+W_{ob}+W_{ob}^{(1)}W_o^{(1)}\right)\mathrm{d}\varphi \tag{48}$$

we can observe that (i) $\psi_{o\eta}\approx-W_o^{(1)}$ is an odd function of φ, consequently (ii) if W_{ob} is an odd function of φ then the above integral vanishes, that is, ε_{mb} is equal to zero. (iii) Otherwise – practically if W_{ob} is an even function φ – ε_{mb} is equal to a constant. We remark that these observations are naturally valid for the case of homogeneous beams as well – see for instance Bradford et al. (2002) and Pi and Bradford (2008).

Consequently: (a) if $\varepsilon_{mb}=$ constant $\neq 0$ we have to solve equation (35) (or, which is the same, equation (47)), (b) if $\varepsilon_{mb}=0$ we have to solve equation

$$W_{ob}^{(4)}+(1+\chi^2)W_{ob}^{(2)}+\chi^2W_{ob}=0\;. \tag{49}$$

It is also important to mention that after buckling every physical quantity is continuous through the interval $\varphi\in[-\vartheta;\vartheta]$ because there is no increment in the loading at $\varphi=0$ – we have assumed that $P_{\zeta\,b}=0$.

The general solution to the inhomogeneous differential equation (47) takes the form

$$W_{ob}(\varphi)=C_1\cos\varphi+C_2\sin\varphi+C_3\sin\chi\varphi+C_4\cos\chi\varphi-\frac{m\varepsilon_{m\,b}}{2\chi^3}\left(\frac{2}{\chi}+A_3\varphi\sin\chi\varphi-A_4\varphi\cos\chi\varphi\right)\;,\quad C_i\in\mathbb{R} \tag{50}$$

while the displacement satisfying differential equation (49) is sought in the form

$$W_{ob}(\varphi)=E_1\cos\varphi+E_2\sin\varphi+E_3\sin\chi\varphi+E_4\cos\chi\varphi\;;\qquad E_i\in\mathbb{R}\;. \tag{51}$$

Here C_i and E_i are undetermined integration constants.

5.2 Pinned-pinned Beam

5.2.1 Antisymmetric and Symmetric Buckling

After the loss of stability the shape of a pinned-pinned curved beam can either be antisymmetric or symmetric with respect to the angle coordinate φ. If the post-buckling shape is [antisymmetric](symmetric) then [$\varepsilon_{mb} = 0$] ($\varepsilon_{mb} \neq 0$). These two possibilities are shown in Figure 3, where a continuous line represents the centerline of the beam in the initial configuration, the dashed line is the pre-buckling shape, while the dotted line is the buckled shape of the centerline.

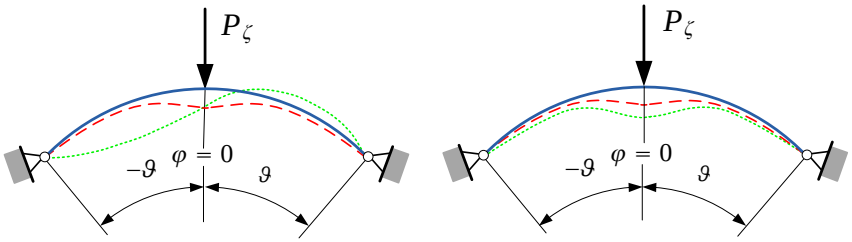

Figure 3: Antisymmetric and symmetric buckling shapes of pinned-pinned beams

5.2.2 Solutions to Antisymmetric Buckling

The boundary conditions in terms of the increments are gathered in Table 2.

Table 2: Boundary conditions in terms of W_{ob} for pinned-pinned beams

Boundary conditions	
Left end	Right end
$W_{ob}(\varphi)\big\|_{\varphi=-\vartheta} = 0$	$W_{ob}(\varphi)\big\|_{\varphi=\vartheta} = 0$
$W_{ob}^{(2)}(\varphi)\Big\|_{\varphi=-\vartheta} = 0$	$W_{ob}^{(2)}(\varphi)\Big\|_{\varphi=\vartheta} = 0$

After substituting solution (51) into the boundary conditions of Table 2 we arrive at a system of linear equations

$$\begin{bmatrix} \cos\vartheta & 0 & 0 & \cos\chi\vartheta \\ 0 & \sin\vartheta & \sin\chi\vartheta & 0 \\ \cos\vartheta & 0 & 0 & \chi^2\cos\chi\vartheta \\ 0 & \sin\vartheta & \chi^2\sin\chi\vartheta & 0 \end{bmatrix} \begin{bmatrix} E_1 \\ E_2 \\ E_3 \\ E_4 \end{bmatrix} = \begin{bmatrix} 0 \\ 0 \\ 0 \\ 0 \end{bmatrix}, \tag{52}$$

which is obviously homogeneous. Nontrivial solution exists if the determinant of the coefficient matrix is zero. In this way we get

$$\mathfrak{D} = (1-\chi)^2(1+\chi)^2 \sin\chi\vartheta \cos\chi\vartheta \cos\vartheta \sin\vartheta = 0\,. \tag{53}$$

Recalling the relation $\chi^2 = 1 - m\varepsilon_m$ we can come to the following conclusions: (a) if $1-\chi = 0$ then $\chi = 1$, consequently $\varepsilon_m = 0$; (b) if $1+\chi = 0$ then $\chi = -1$ and so $\varepsilon_m > 0$; (c) if $\sin\chi\vartheta = 0$ then $\chi = \pi/\vartheta$ and (d) if $\cos\chi\vartheta = 0$ then $\chi = \pi/2\vartheta$. We remark that cases (a) and (b) have no physical sense. There belongs no bifurcation buckling to solution (d) since then $W_{ob}(\varphi) = E_4\cos\frac{\pi}{2\vartheta}\varphi$, it follows from (48) that $\varepsilon_{mb} \neq 0$. This means that the critical axial strain for bifurcation buckling is

$$\varepsilon_m = \frac{1}{m}\left(1-\chi^2\right) = \frac{1}{m}\left[1-\left(\frac{\mathfrak{G}(\vartheta)}{\vartheta}\right)^2\right], \qquad \text{where} \qquad \mathfrak{G}(\vartheta) = \pi\,. \tag{54}$$

If we now substitute solution (c) back into the equation system (52) we can easily check that $E_1 = E_2 = E_4 = 0$. Consequently, it follows from the general solution (51) that the shape of the beam is

$$W_{ob}(\varphi) = E_3 \sin\frac{\pi}{\vartheta}\varphi\,. \tag{55}$$

This function is antisymmetric in terms of the angle coordinate φ.

Note that if we neglect the effect of the angle of rotation on the axial strain then we shall change the notation ε_{mb} to $\varepsilon_{o\xi\, b}$.

5.2.3 Solutions to Symmetric Buckling

For symmetric buckling $\varepsilon_{mb} \neq 0$. When solving the differential equation (47) it is clearly sufficient to consider a half of the beam. For the right half of the beam the boundary conditions are presented in Table 3.

Table 3: Boundary conditions for the pinned-pinned beam assuming a symmetric buckling shape

Boundary conditions	
Crown point	Right end
$W_{ob}^{(1)}(\varphi)\Big\vert_{\varphi=0} = 0$	$W_{ob}(\varphi)\,\vert_{\varphi=\vartheta} = 0$
$W_{ob}^{(3)}(\varphi)\Big\vert_{\varphi=0} = 0$	$W_{ob}^{(2)}(\varphi)\Big\vert_{\varphi=\vartheta} = 0$

Upon substitution of solution (50) into the boundary conditions we arrive at the following inhomogeneous system of linear equations

$$\begin{bmatrix} 0 & -2\chi^3 & -2\chi^4 & 0 \\ 0 & -2\chi & -2\chi^4 & 0 \\ \cos\vartheta & \sin\vartheta & \sin\chi\vartheta & \cos\chi\vartheta \\ 2\chi^2\cos\vartheta & 2\chi^2\sin\vartheta & 2\chi^4\sin\chi\vartheta & 2\chi^4\cos\chi\vartheta \end{bmatrix} \begin{bmatrix} C_1 \\ C_2 \\ C_3 \\ C_4 \end{bmatrix} = \\ = m\varepsilon_{mb} \begin{bmatrix} A_4 \\ 3A_4 \\ \frac{1}{2\chi^3}\left(\frac{2}{\chi} + A_3\vartheta\sin\chi\vartheta - A_4\vartheta\cos\chi\vartheta\right) \\ A_3\left(\chi\vartheta\sin\chi\vartheta - 2\cos\chi\vartheta\right) - A_4\left(2\sin\chi\vartheta + \vartheta\chi\cos\chi\vartheta\right) \end{bmatrix}, \quad (56)$$

which can be solved in a closed form – the solutions are presented in Section A.1.7, where the decomposition of these constants into two parts, one independent of $\mathcal{P}$ and the other depending linearly on $\mathcal{P}$, are also shown – see equations (A.30), (A.31), (A.32) and (A.33) for details.

The solution to W_{ob} can now be given in terms of the new constants $\hat{C}_{ij}$ as follows – see equations (A.32) for further details –

$$W_{ob} = \varepsilon_{mb}\left[\left(\hat{C}_{01} + \hat{C}_{11}\cos\varphi + \hat{C}_{41}\cos\chi\varphi + \hat{C}_{51}\varphi\sin\chi\varphi\right) + \right. \\ \left. + \frac{\mathcal{P}}{\vartheta}\left(\hat{C}_{12}\cos\varphi + \hat{C}_{22}H\sin\varphi + \hat{C}_{32}H\sin\chi\varphi + \hat{C}_{42}\cos\chi\varphi + \hat{C}_{52}\varphi\sin\chi\varphi + \hat{C}_{62}H\varphi\cos\chi\varphi\right)\right]. \quad (57)$$

With the knowledge of the radial displacement we can determine the rotation increment

$$-\psi_{o\eta\, b} \simeq W_{ob}^{(1)} = \varepsilon_{mb}\left[K_{11}\sin\varphi + K_{41}\sin\chi\varphi + K_{51}\varphi\cos\chi\varphi + \right. \\ \left. + \left(K_{12}\sin\varphi + K_{22}\cos\varphi + K_{32}\cos\chi\varphi + K_{42}\sin\chi\varphi + K_{52}\varphi\cos\chi\varphi + K_{62}\chi\varphi\sin\chi\varphi\right)\frac{\mathcal{P}}{\vartheta}\right], \quad (58)$$

where

$$K_{11} = -\hat{C}_{11}\,, \qquad K_{41} = \hat{C}_{51} - \hat{C}_{41}\chi\,, \qquad K_{51} = \hat{C}_{51}\chi\,, \qquad K_{12} = -\hat{C}_{12}\,, \qquad K_{22} = \hat{C}_{22}H\,, \\ K_{32} = \hat{C}_{32}H\chi + \hat{C}_{62}H\,, \qquad K_{42} = \hat{C}_{52} - \hat{C}_{42}\chi\,, \qquad K_{52} = \hat{C}_{52}\,, \qquad K_{62} = -\hat{C}_{62}H \quad (59)$$

are the coefficients that have been introduced for the sake of brevity. If we neglect the effect of the tangential displacement on the angle of rotation – this is an assumption – then equation (48) can be rewritten as

$$\varepsilon_{mb} = \frac{1}{\vartheta}\int_0^{\vartheta}\left(W_{ob} + W_o^{(1)}W_{ob}^{(1)}\right)\mathrm{d}\varphi\,. \quad (60)$$

If we now substitute (42), (57) and (58) into equation (60) then, after performing the integrations, we get

$$1 = \left[I_{01} + \frac{\mathcal{P}}{\vartheta} I_{02} \right] + \left[I_{11} + \frac{\mathcal{P}}{\vartheta} I_{12} + \left(\frac{\mathcal{P}}{\vartheta} \right)^2 I_{13} \right]$$

or what is the same

$$I_{13} \left(\frac{\mathcal{P}}{\vartheta} \right)^2 + [I_{02} + I_{12}] \frac{\mathcal{P}}{\vartheta} + [I_{01} + I_{11} - 1] = 0 \, ; \qquad I_{ij} \in \mathbb{R} \, . \tag{61}$$

Here the constants I_{01} and I_{02} follow from the first integral in (60), while the coefficients I_{11}, I_{12} and I_{13} are from the second one. We can therefore remark that closed form solutions of the integrals are again possible. Some details just to provide the validity of this statement are gathered in Subsection A.1.8. However, within the framework of this article it is not possible to list all the part integrals, which constitute I_{11}, I_{12} and I_{13} since their closed forms are long expressions requiring a bunch of space, which is not available. We also remark that we used an IMSL subroutine – its name is `DQDAG` – to compute the value of the integrals in question when we determined the critical load.

6 Computational Results

6.1 Pinned-pinned Beam

As it has already been mentioned that pinned-pinned circular beams can buckle in an antisymmetric mode (with no strain increment) and also in a symmetric mode (given that the length of the centerline changes during the phenomenon). Our aim is to compare the outcomes of our model to those derived in Bradford et al. (2002). Since the present model keeps some terms the cited authors have neglected, we expect improved results for the critical loads and an extended range of applicability with regard to the central angle of the beam. The results of Bradford et al. (2002) – in a comparison with finite element calculations – seem to be fairly accurate as long as $\vartheta < \pi/4$. However, we are evaluating the cited model for greater central angles as well to make the differences more spectacular. To facilitate the evaluation process – following the footsteps of Bradford et al. – let us introduce the parameter

$$\lambda = \sqrt{\frac{A_e \rho_o^2}{I_{e\eta}}} \vartheta^2 = \sqrt{m} \vartheta^2, \tag{62}$$

which is referred to as the modified slenderness ratio of the beam.

Altogether we can distinguish four different intervals regarding the stability of pinned-pinned shallow beams. The endpoint of each interval is a function of the parameter m as $\lambda = \lambda(m)$. For the most shallow beams (which behave like columns) there is no loss of stability, i.e. such structural members act as straight beams loaded transversally. With λ increasing emerges the possibility of symmetric (or limit point or snap-through) buckling: $W_{ob}(\varphi) = W_{ob}(-\varphi)$. After that both symmetric and antisymmetric (or bifurcation) buckling might occur but meanwhile in the third notable interval the symmetric shape governs, in the fourth one (with even greater values of λ) antisymmetric buckling is the dominant type. Based on what has been mentioned, in Table 4 we have collected the typical ranges (with limits rounded to two decimal numbers) for four different magnitudes of the parameter m in terms of λ.

Table 4: Buckling modes of pinned-pinned beams

m				
1 000	10 000	100 000	1 000 000	
$\lambda < 3.80$	$\lambda < 3.87$	$\lambda < 3.89$	$\lambda < 3.90$	no buckling
$3.80 < \lambda < 7.90$	$3.87 < \lambda < 7.96$	$3.89 < \lambda < 7.97$	$3.90 < \lambda < 7.97$	limit point only
$7.90 < \lambda < 9.68$	$7.96 < \lambda < 10.05$	$7.97 < \lambda < 10.18$	$7.97 < \lambda < 10.23$	bifurcation point after limit point
$\lambda > 9.68$	$\lambda > 10.05$	$\lambda > 10.18$	$\lambda > 10.23$	bifurcation point before limit point

The approximative polynomials defining the boundaries of all these intervals are presented in the forthcoming and are compared to those achieved by Bradford et al. The results of them do not depend on the parameter m. The lower limit for antisymmetric buckling is obtained from the condition that the slenderness must be real, i.e. by

setting the discriminant of (46) to zero when $\chi\vartheta = \pi$, therefore

$$\lambda(m) = \begin{cases} 7.975\,6 + 5.4 \cdot 10^{-7} m - 2.15/m^{0.5} & \text{if} \quad m \in [1\,000; 10\,000] \\ 7.971\,4 + 1.33 \cdot 10^{-8} m - 118.14/m - 6.636 \cdot 10^{-15}\, m^2 & \text{if} \quad m \in [10\,000; 1\,000\,000] \\ 7.96 & \text{by} \quad \text{Bradford et al. (2002) p. 714.} \end{cases}$$

The difference to the previous model is significant if m is small, otherwise they almost coincide when $m > 5\,000$.

Proceeding with the lower limit of symmetric buckling we can write the approximative polynomial as

$$\lambda(m) = \begin{cases} 3.903\,1 + 8.14 \cdot 10^{-8} m - 3.05/m^{0.5} & \text{if } m \in [1\,000; 10\,000] \\ \dfrac{11.3 \cdot 10^5}{m^2} - \dfrac{357}{m} + 3.897\,471 + 9.1725 \cdot 10^{-9}\, m - 5.295 \cdot 10^{-15}\, m^2 & \text{if } m \in [10\,000; 1\,000\,000] \\ 3.91 & \text{by Bradford et al.} \end{cases}$$

It is again close to that achieved by Bradford et al. when $m > 3\,000$, and it turns out that the limit value is actually the same.

For pinned-pinned shallow curved beams there is an intersection point of the symmetric and antisymmetric buckling curves. At this point the critical load for symmetric and antisymmetric buckling coincide, i.e., there is a switch between limit point and bifurcation buckling. The equation of the fitting curve is

$$\lambda(m) = \begin{cases} -271/m + 9.923 + 2.84 \cdot 10^{-5}\, m - 1.2 \cdot 10^{-9}\, m^2 & \text{if} \quad m \in [1\,000; 10\,000] \\ \dfrac{7.162 \cdot 10^6}{m^2} - \dfrac{2144}{m} + 10.200\,3 + 7.7 \cdot 10^{-8}\, m - 4.549 \cdot 10^{-14}\, m^2 & \text{if} \quad m \in [10\,000; 1\,000\,000] \\ 9.8 & \text{by Bradford et al.} \end{cases}$$

The limit value of our solution is $\lambda \approx 10.2$ if m is sufficiently great, and this is again close but different by 4% from the limit of the earlier model.

6.1.1 Antisymmetric Loss of Stability

Pinned-pinned shallow beams may buckle in an antisymmetric (bifurcation) mode for which there is no strain increment. The loss of stability occurs when the strain reaches the lowest critical strain level, which is $\chi\vartheta = \pi$. Substituting it into the pre-buckling equilibrium equation (46) we can solve it for the dimensionless critical load. The numerical results are presented graphically in Figure 4 for four different magnitudes of m. Our results are

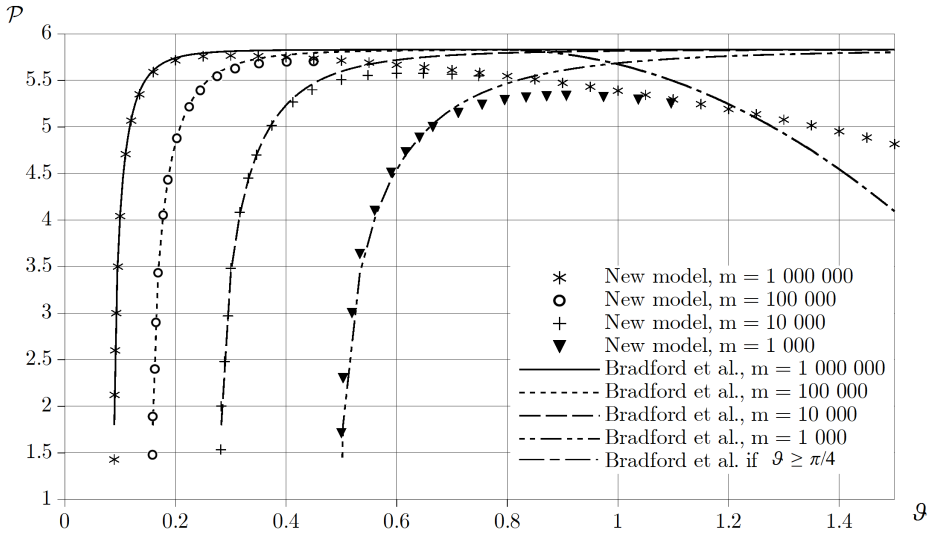

Figure 4: Antisymmetric dimensionless buckling load against the semi-vertex angle

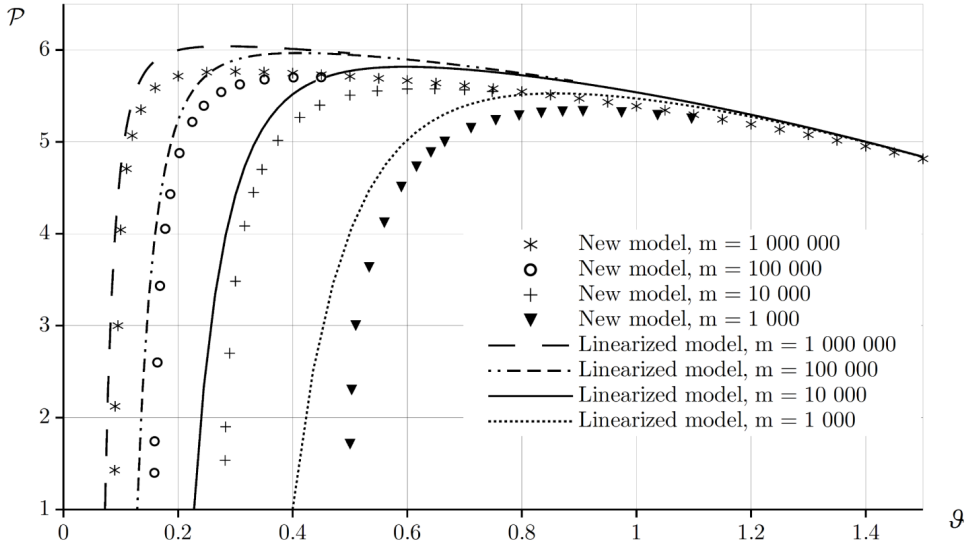

Figure 5: Antisymmetric buckling load – nonlinear versus linearized model

compared to those of Bradford et al. (2002). It can clearly be seen that for any fixed parameter m the two models yield similar results around the lower limit of antisymmetric buckling. It is also visible that the limit values for the two models are not functions of m. That is the reason why we have drawn only the asterisk symbols throughout the plotted interval. The maximum difference is at most about 4.7% from each other if $\vartheta = \pi/4$ (so the beam is still shallow) and it is approximately 14% if $\vartheta = 1.4$ (the beam is not shallow). What is of more importance is that the new model yields quite the same or lower buckling loads – i.e. the earlier model generally overestimates a bit the load such structural members can bear.

We have to mention that in Bradford et al. (2002) a formula is published – see equation (59) in the paper cited – which approximates the critical load if $\vartheta \geq \pi/4$. It turns out to be a function of the central angle only. In their article Bradford et al. mention that it coincides well with finite element calculations for any investigated value of m. We have also plotted this relation in Figure 4. Compared to our model it yields greater critical loads if $\vartheta \in [0.78; 1.23]$. After the intersection point at $\vartheta = 1.23$ this tendency changes and at the right end of the interval the difference reaches up to 15%. We must however mention that it is not clear how and under what assumptions Bradford et al. have obtained this polynomial.

The curves shown for the critical load in Figure 4 – antisymmetric stability loss – can be approximated with a good accuracy by the following functions:

$$\mathcal{P}(m = 1\,000\,000, \vartheta) = \begin{cases} 0.85\vartheta + 5.615 - 1.66 \cdot 10^{-5}/\vartheta^5 - 1.321 \cdot 10^{-42}/\vartheta^{40} & \text{if} \quad \vartheta \in [0.09; 0.2] \\ -0.004\,2/\vartheta^2 + 5.85 - 0.45\,\vartheta^2 & \text{if} \quad \vartheta \in [0.21; 1.5] \end{cases} \tag{63a}$$

$$\mathcal{P}(m = 100\,000, \vartheta) = \begin{cases} -1.5 \cdot 10^{-6}/\vartheta^8 + 5.13 + 1.62\,\vartheta & \text{if} \quad \vartheta \in [0.158; 0.34] \\ -0.061/\vartheta + 5.93 - 0.48\,\vartheta^2 & \text{if} \quad \vartheta \in [0.341; 1.5] \end{cases} \tag{63b}$$

$$\mathcal{P}(m = 10\,000, \vartheta) = \begin{cases} -7.5 \cdot 10^{-7}/\vartheta^{12} - 1.96/\vartheta^{0.5} + 8.33 & \text{if} \quad \vartheta \in [0.281; 0.465] \\ -0.64/\vartheta + 7.55 - 1.53\,\vartheta & \text{if} \quad \vartheta \in [0.466; 1.5] \end{cases} \tag{63c}$$

$$\mathcal{P}(m = 1\,000, \vartheta) = \begin{cases} -7.6 \cdot 10^{-5}/\vartheta^{15} - 3.44/\vartheta^{0.5} + 9.24 & \text{if} \quad \vartheta \in [0.498; 0.75] \\ -3.153\,6\vartheta + 13.888\,4 - 5.424/\vartheta^{0.5} - 4.034 \cdot 10^{-4}/\vartheta^{15} & \text{if} \quad \vartheta \in [0.76; 1.5]\,. \end{cases} \tag{63d}$$

It might be interesting to check what results the model that is linear in $\mathcal{P}$ returns for the critical load. Since the critical strain $\chi\vartheta = \pi$ is still valid for this case, upon substituting it into the linearized and averaged strain (44) we can carry out the evaluation. As can be seen from Figure 5 the buckling limits are different and the linearized model generally overestimates the buckling load. The difference is always less than 8% when it is compared to the nonlinear model and it decreases as ϑ increases.

6.1.2 Symmetric Buckling and FEM Verifications

A symmetric buckling shape can only occur with a strain increment different from zero. This problem is a little more difficult than the previous one since we are neither aware of the critical axial strain ε_m (or what is the same the critical χ) nor of the critical load $\mathcal{P}$. Equation (61) for the post-buckling state is valid only for symmetric buckling while the pre-buckling relation (46) always holds. Consequently, these two nonlinear equations should be solved together to get the two unknowns.

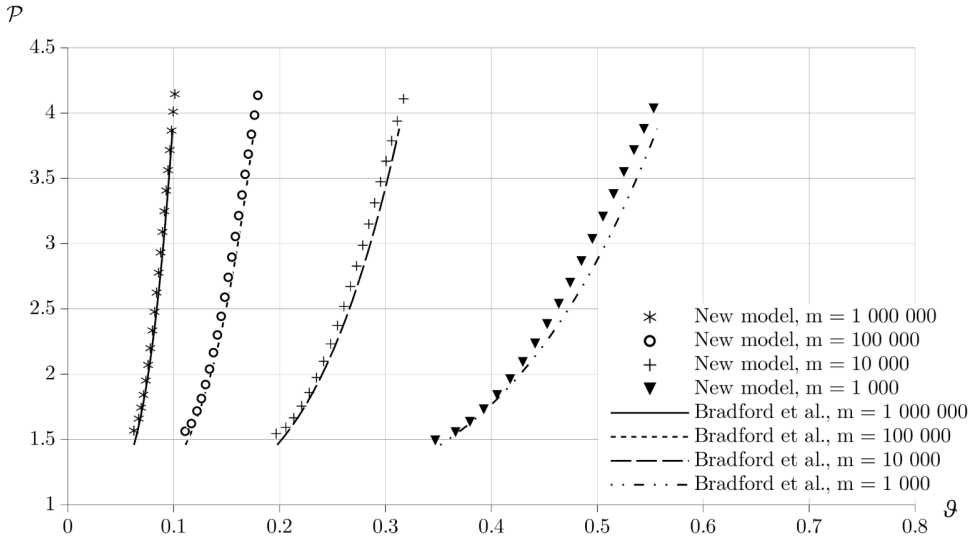

Figure 6: Symmetric buckling load against the semi-vertex angle

Results between the lower and upper endpoints of the corresponding intervals, in which a symmetric buckling shape governs, are shown in Figure 6. It is clear that if m is sufficiently great there is hardly any noticeable difference between the two models (except the endpoints). However, if $m = 1\,000$ the maximum difference is up to 10%, which is substantial as the length of this interval is only ~ 0.22 in ϑ. It is interesting to remark that this time the more accurate model always predicts greater critical loads.

Here we present the approximative functions for the symmetric buckling load of pinned-pinned beams. These are valid till the intersection point of the symmetric and antisymmetric buckling curves is reached

$$\mathcal{P}(m,\vartheta) = \begin{cases} 0.546/\vartheta - 16.8 + 154\,\vartheta & \text{if} \quad m = 1\,000\,000 \\ 0.98/\vartheta - 16.98 + 87.4\,\vartheta & \text{if} \quad m = 100\,000 \\ 1.8/\vartheta - 17.53 + 50.4\,\vartheta & \text{if} \quad m = 10\,000 \\ 3.4/\vartheta - 18.8 + 30.2\,\vartheta & \text{if} \quad m = 1\,000\,. \end{cases} \tag{64}$$

It would be again possible to compare the former results to those available via the linearized model governed by relations (43) and (A.38). This simplified model however yields such critical loads, which are considerably greater than the more accurate ones. Therefore it makes no sense to compare them numerically.

Some control computations were carried out for the in-plane symmetric snap-through buckling of curved beams using the commercial finite element softwares Abaqus 6.7. and ADINA 8.9. The cross-section considered is rectangular with $0.01\,[m]$ width and $0.005\,[m]$ height and the Young's modulus is $2 \times 10^{11}\,[Pa]$. In Abaqus we have used $B22$ elements and the Static,Riks step. In ADINA 2-node beam elements and Collapse Analysis have been applied. All the numerical results are gathered in Table 5. Our results coincide with or are very close to those of Abaqus and ADINA and are more accurate in this comparison than the results published in Bradford et al. (2002).

Table 5: Comparison with FE calculations – symmetric shape

m	λ	$\mathcal{P}_{New\,model}$	$\mathcal{P}_{Bradford\,et\,al.}$	$\mathcal{P}_{Abaqus}$	$\mathcal{P}_{ADINA}$
1 000	4.56	1.63	1.62	1.68	1.7
1 000	5.84	2.09	2.02	2.11	2.12
1 000	7.76	3.03	2.8	2.97	3
1 000	8.72	3.55	3.28	3.43	3.49
1 000	9.36	3.87	3.62	3.72	3.82
1 000 000	4.48	1.66	1.6	1.66	1.66
1 000 000	5.44	1.95	1.88	1.95	1.95
1 000 000	7.36	2.77	2.62	2.77	2.77
1 000 000	9.6	3.86	3.76	3.87	3.86

A few control calculations for the antisymmetric buckling load were also performed under Abaqus. We have used the same cross-section, material, element type and step as before. Initial geometric imperfections were introduced to the model via the first antisymmetric buckling mode of the beams, obtained from the Linear perturbation, Buckle step. All the corresponding data are collected in Table 6. We can conclude that our model and that of Abaqus show a good correlation for the tested beams. The new model generally allows lower loads, but the difference is always below $6,5\%$, even when λ is greater.

Table 6: Comparison with FE calculations – antisymmetric shape

m	λ	$\mathcal{P}_{New\,model}$	$\mathcal{P}_{Bradford\,et.\,al}$	$\mathcal{P}_{Abaqus}$	imperfection
1 000	487.38	5.11	5.18	5.19	$1.275 \cdot 10^{-4}$
1 000	1096.62	5.28	5.70	5.46	$1.912 \cdot 10^{-4}$
1 000	1713.47	5.05	5.78	5.40	$5.73 \cdot 10^{-4}$
1 000 000	121.85	5.76	5.82	5.82	$1.975 \cdot 10^{-5}$
1 000 000	761.54	5.49	5.83	5.61	$3.686 \cdot 10^{-3}$
1 000 000	1492.63	5.17	5.83	5.38	$1.85 \cdot 10^{-2}$

6.1.3 Load-crown Point Displacement Curves

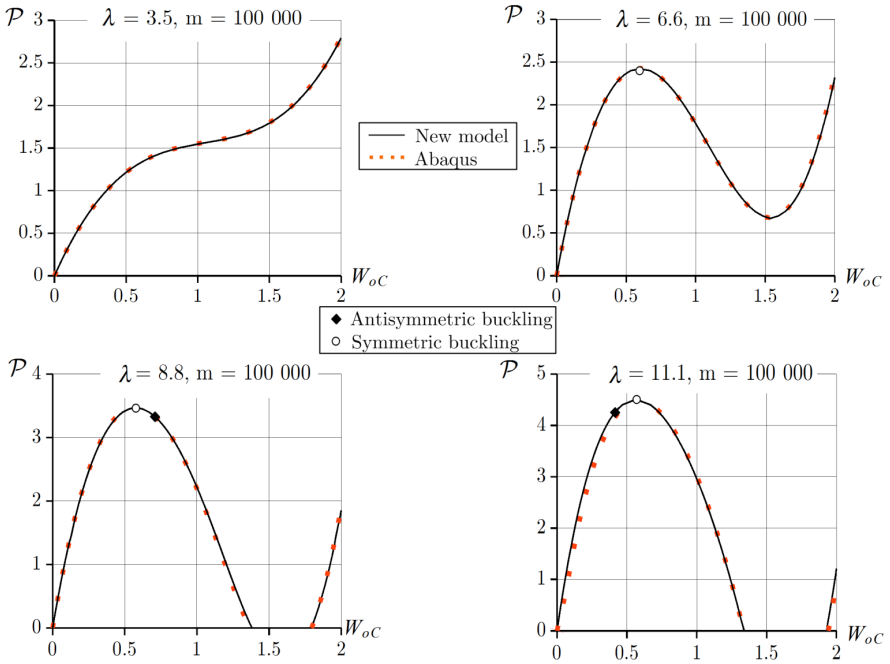

Figure 7: Dimensionless load versus displacement of the crown point

Choosing $m = 100\,000$ we have drawn the primary equilibrium paths for four different values of λ, or what is the same, four different semi-vertex angles were picked. The reason is that there belongs a different path type to

each geometry. In Figure 7 the dimensionless concentrated force $\mathcal{P}$ is plotted against the dimensionless vertical displacement W_{oC} at the crown point. The former quantity is obtained upon dividing the displacement by the initial rise of the curved beam so that

$$W_{oC} = -\frac{W_o|_{\varphi=0}}{(1-\cos\vartheta)} \,. \tag{65}$$

If $\lambda = 3.5$ ($\vartheta \simeq 0.105$) the slope of the corresponding curve is positive for any $\mathcal{P} > 0$ and so there is no buckling. When λ is 6.6 ($\vartheta \simeq 0.144$) symmetric limit point buckling occurs at $\mathcal{P} \simeq 2.4$. The condition of finding this point is $\partial\mathcal{P}/\partial W_{oC} = 0$. If $\lambda = 8.8$ ($\vartheta \simeq 0.166$) it can be seen that a bifurcation point appears but on the descending branch of the deflection curve. Thus the critical behavior is still represented by the limit point. Finally, for $\lambda = 11.1$ ($\vartheta \simeq 0.187$) shortly before the limit point there is a bifurcation point, so we expect an antisymmetric buckled shape. The bifurcation and limit points coincide when $\lambda \simeq 10.18$ ($\vartheta \simeq 0.179$). The results are almost identical with those obtained by Abaqus.

Figure 8 shows how the dimensionless load varies with the ratio $\varepsilon_m/\varepsilon_{m,\,cr,\,a}$ when $m = 100\,000$. Here $\varepsilon_{m,\,cr,\,a}$ is the critical strain for antisymmetric buckling. For $\lambda = 3.5$ there are two different values of $\mathcal{P}$, which only occur once for any ε_m. The strain ratio is always less than the critical value. When λ is 6.6 starting from the origin we can see a point in which, $\partial\mathcal{P}/\partial(\varepsilon_m/\varepsilon_{m,\,cr\,a}) = 0$, so the tangent is zero. To this point belongs symmetric snap-through buckling. The critical antisymmetric strain is, however, out of reach. When $\lambda = 8.8$ we experience that the path crosses the critical antisymmetric strain, but before that there is a limit point so the latter one dominates. Finally, for $\lambda = 11.1$ the bifurcation point comes prior to the limit point and, thus, antisymmetric buckling shape is expected. It is also worth pointing out that independently of λ one branch always starts from the origin while the other one commences somewhere between $\mathcal{P}(\lambda) \simeq 2.9 \ldots 3.1$. At the point where $\mathcal{P} \simeq \pi/2$ and $\vartheta \simeq 0.248$, the branches intersect each other.

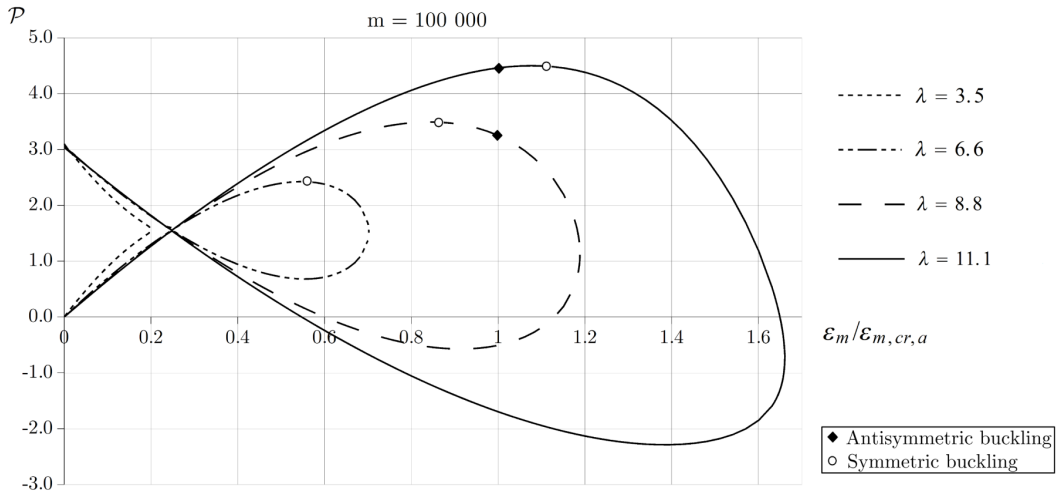

Figure 8: Dimensionless load – strain graphs

7 The Effect of Heterogeneity on the Buckling Load

In this section we would like to demonstrate how heterogeneity affects the buckling load of bilayered beams with rectangular cross-section, given that the overall geometry remains unchanged. As can be seen in Figure 9, the upper layer has a Young's modulus of E_1 and a height of y. The height is a parameter – it varies in the interval $[0, b]$. When $y = 0$, the beam is homogeneous with a Young's modulus of E_2 and a heterogeneity parameter m_2. If $y = b$, the homogeneous cross-section has a Young's modulus E_1 and a heterogeneity parameter m_1. For any other (and obviously heterogeneous) distributions, this time, we use the notation m_{12}. Making use of equations (9a), (9b) and (12), we can plot the fraction m_{12}/m_2 – which is a function of E_2/E_1 only if y is fixed – against y/b. Some results are shown in Figure 10.

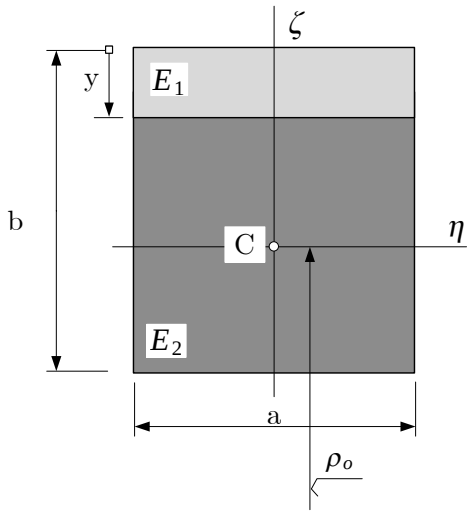

Figure 9: The investigated bilayered cross-section

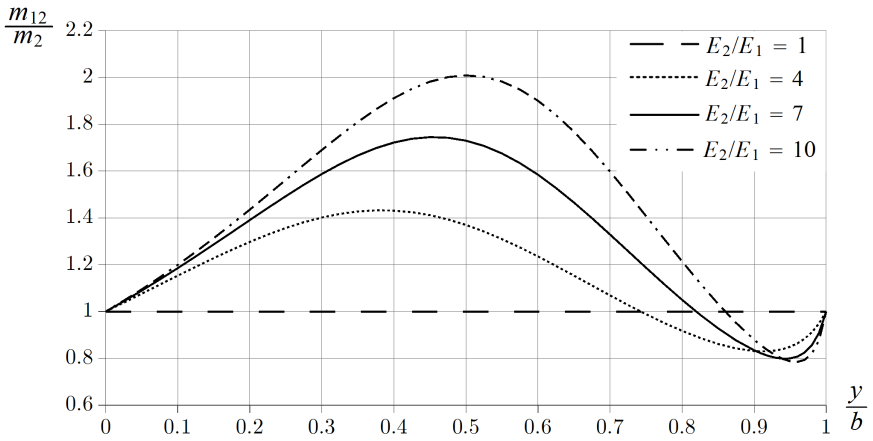

Figure 10: The effects of y on the inhomogeneity parameter m

We now present some simple numerical examples to find out the influence of the heterogeneity on the antisymmetric buckling load. We chose antisymmetric buckling, because it is the dominant mode for the majority of pinned-pinned beams. Let E_2/E_1 be 4. Then the quotient m_{12}/m_2 has a maximum at $y = 0.383$, that is ~ 1.4324 – we refer back to Figure 10.

Further, let m_2 be $1\,000$ – we remark that m_2 belongs to the homogeneous beam. Given that the geometry of the beam is unchanged (except for the height of the layers), the maximum of m_{12} due to the heterogeneity is $1\,432.4$. We now evaluate how the critical load depends on the heterogeneity according to the nonlinear theory. We have chosen two distant semi-vertex angles (0.55 and 1.2) to briefly demonstrate the effects of ϑ. These are close to the endpoints of the corresponding curve in Figure 4 and, therefore, might illustrate well the range in which the load can vary.

For both semi-vertex angles we find that the heterogeneity has a massive effect on the critical load – see Figure 11 in which, $P_{\zeta\,\mathrm{hom}}$ is the critical load of homogeneous cross-section, and $P_{\zeta\,\mathrm{het}}$ denotes that of the heterogeneous bilayered cross-section. We can conclude that the greater the heterogeneity is, the greater its effect on the buckling load is. At the maximum of m_{12}/m_2, that is, at 1.432, the critical load has a minimum: it decreases to the $(52 \ldots 58)\%$ of the critical load valid for homogeneous beams with the investigated central angles.

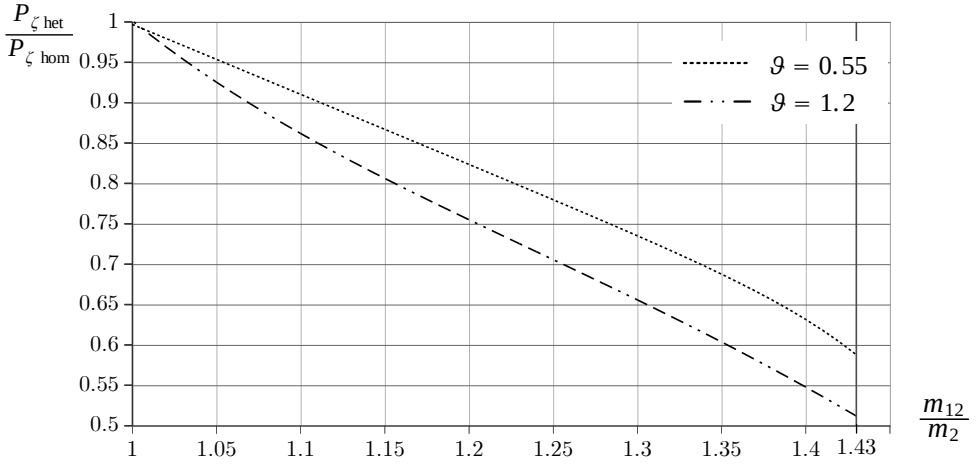

Figure 11: The effect of heterogeneity to the critical load when $m_2 = 1\,000$

We have also checked the case when m_2 is $1\,000\,000$. We picked $\vartheta = 0.1$ and 1.2, for the same reason as before. Compared to the previous geometries, very similar computational results were obtained. These are provided in Figure 12.

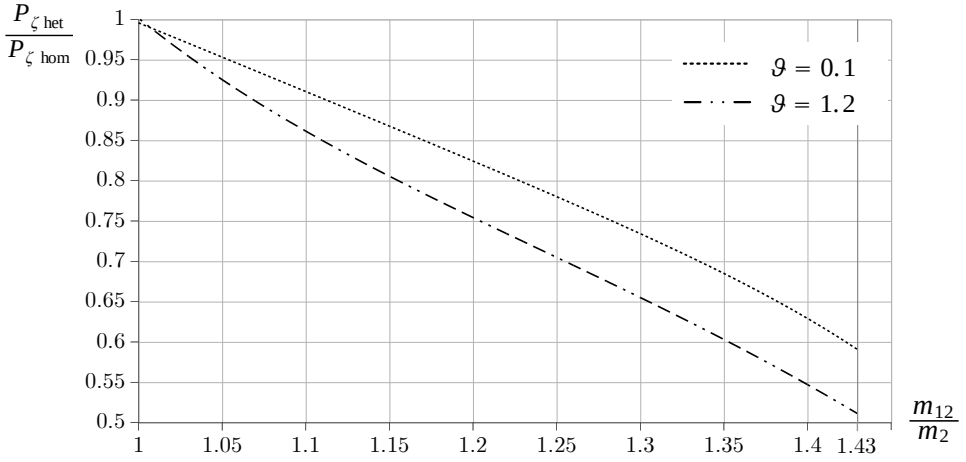

Figure 12: The effect of heterogeneity to the critical load when $m_2 = 1\,000\,000$

The latter two figures illustrate well how huge impact heterogeneity on the admissible load of pinned-pinned curved beams can have.

8 Concluding Remarks

Under the assumption of cross-sectional inhomogeneity we have derived differential equations both for the pre-buckling radial displacements – see equation (28) – and for the post-buckling radial displacements – see equation (35) for symmetric buckling and equation (49) for asymmetric buckling. The cross-sectional inhomogeneity is implied in these equations via the parameter χ, i.e., via the parameter m – compare equations (9), (12) and $(28)_2$. We remark that equations (28) and (35) are more accurate than equations (29) and (36) solved by Bradford et al. (2002). Though we neglected the effect of the tangential displacement on the angle of rotation – paper by Bradford et al. (2002) also makes this assumption – we had expected, with a regard to the more accurate problem (formulation) set up that the results for the critical load would be more accurate than those published in Bradford et al. (2002) and we also hoped that they would be valid for greater central angles.

According to the computational results, there are four intervals in which (a) there is no buckling, (b) limit point buckling occurs, (c) there is a bifurcation point after the limit point, (d) the bifurcation point precedes the limit point. The endpoints of these intervals are not constant but depend on λ. The difference with respect to the previous model is considerable if m is small, otherwise the endpoints almost coincide with those published by

Bradford et al. (2002) if $m > 5\,000$.

If the buckling is *antisymmetric* then for (a) $m = 1\,000$ and $\vartheta \in (0.7, 1.4)$, (b) $m = 10\,000$ and $\vartheta \in (0.47, 1.4)$, (c) $m = 100\,000$ and $\vartheta \in (0.4, 1.4)$, (d) $m = 1000\,000$ and $\vartheta \in (0.3, 1.4)$ our results are different from those published in Bradford et al. (2002) – see Figure 4 for details. The greater ϑ is the greater the difference is. The maximum difference is about 14% if $\vartheta = 1.4$. We also remark that the new model yields the same or lower buckling loads – i.e. the earlier model generally overestimates a bit the load such structural members can bear.

It is worth mentioning that the model linearized in $\mathcal{P}$ provides similar results, which are, in general, greater than the results of the nonlinear model – see Figure 5 for a comparison.

If the buckling is *symmetric* then – as can bee seen from Figure 6 – our results are closer to those published by Bradford at al. If $m = 1\,000$ the maximum difference is up to 10%, which is substantial as the size of this interval is only ~ 0.22 in ϑ. It is also interesting to remark again that this time the more accurate model always predicts greater permissible loads.

Figures 11 and 12 illustrate well how great effect heterogeneity can have on the critical load of bilayered rectangular cross-sections.

More accurate models. In what follows we mention two possibilities.
(i) First we remind the reader of the fact that we have neglected the last term in the equilibrium equation

$$\frac{\mathrm{d}N_b}{\mathrm{d}s} + \frac{1}{\rho_o}\frac{\mathrm{d}M_b}{\mathrm{d}s} - \frac{1}{\rho_o}\underbrace{\left(N + \frac{M}{\rho_o}\right)}_{A_e\varepsilon_m}\psi_{o\eta\, b} = 0 \tag{66}$$

– for the sake of a comparison see equation (34) that follows from (31a). It is also worth mentioning that the negligence mentioned is generally accepted in the literature. In what follows we shall keep this term.

If we recall equation (31b) in which we neglect the terms quadratic in the increments ($f_{nb} = 0$ for our problem) and assume here and in what follows that $A_e\varepsilon_m$ is constant, then we have

$$\frac{\mathrm{d}^2M_b}{\mathrm{d}s^2} - \frac{N_b}{\rho_o} - \underbrace{\left(N + \frac{M}{\rho_o}\right)}_{A_e\varepsilon_m}\frac{\mathrm{d}\psi_{o\eta\, b}}{\mathrm{d}s} - \underbrace{\left(N_b + \frac{M_b}{\rho_o}\right)}_{A_e\varepsilon_{mb}}\frac{\mathrm{d}\psi_{o\eta}}{\mathrm{d}s} + \psi_{o\eta}\frac{\mathrm{d}}{\mathrm{d}s}\underbrace{\left(N_b + \frac{M_b}{\rho_o}\right)}_{A_e\varepsilon_{mb}} = 0\,. \tag{67}$$

Substitute the derivative $\mathrm{d}N_b/\mathrm{d}s + \mathrm{d}M_b/(\rho_o\mathrm{d}s)$ from equation (66) into the last term on the left side of this equation and ignore the resulting cubic term. If we derive the equation obtained in this way with respect to s we get

$$\rho_o\frac{\mathrm{d}^3M_b}{\mathrm{d}s^3} - \frac{\mathrm{d}N_b}{\mathrm{d}s} - \rho_o\underbrace{\left(N + \frac{M}{\rho_o}\right)}_{A_e\varepsilon_m}\frac{\mathrm{d}^2\psi_{o\eta\, b}}{\mathrm{d}s^2} - \rho_o\underbrace{\left(N_b + \frac{M_b}{\rho_o}\right)}_{A_e\varepsilon_{mb}}\frac{\mathrm{d}^2\psi_{o\eta}}{\mathrm{d}s^2} + \rho_o\frac{\mathrm{d}\psi_{o\eta}}{\mathrm{d}s}\frac{\mathrm{d}}{\mathrm{d}s}\underbrace{\left(N_b + \frac{M_b}{\rho_o}\right)}_{A_e\varepsilon_{mb}} = 0\,. \tag{68}$$

The last term on the left side is again a cubic one therefore it can be neglected – the reasoning is the same as before. If we drop this term and add the result

$$\rho_o\frac{\mathrm{d}^3M_b}{\mathrm{d}s^3} - \frac{\mathrm{d}N_b}{\mathrm{d}s} - \rho_o\underbrace{\left(N + \frac{M}{\rho_o}\right)}_{A_e\varepsilon_m}\frac{\mathrm{d}^2\psi_{o\eta\, b}}{\mathrm{d}s^2} - \rho_o\underbrace{\left(N_b + \frac{M_b}{\rho_o}\right)}_{A_e\varepsilon_{mb}}\frac{\mathrm{d}^2\psi_{o\eta}}{\mathrm{d}s^2} = 0 \tag{69}$$

to equation (66) then we have

$$\rho_o\frac{\mathrm{d}^3M_b}{\mathrm{d}s^3} + \frac{1}{\rho_o}\frac{\mathrm{d}M_b}{\mathrm{d}s} - \frac{1}{\rho_o}\underbrace{\left(N + \frac{M}{\rho_o}\right)}_{A_e\varepsilon_m}\psi_{o\eta\, b} - \rho_o\underbrace{\left(N + \frac{M}{\rho_o}\right)}_{A_e\varepsilon_m}\frac{\mathrm{d}^2\psi_{o\eta\, b}}{\mathrm{d}s^2} - \rho_o\underbrace{\left(N_b + \frac{M_b}{\rho_o}\right)}_{A_e\varepsilon_{mb}}\frac{\mathrm{d}^2\psi_{o\eta}}{\mathrm{d}s^2} = 0\,. \tag{70}$$

For antisymmetric buckling we can assume that $\varepsilon_{mb} \simeq \varepsilon_{o\xi\, b} = U^{(1)}_{ob} + W_{ob} = 0$. Utilizing now the kinematic equation $(15)_2$ for $\psi_{o\eta\, b}$ and Hooke's law (20) for M_b we get

$$\left(U^{(6)}_{ob} + U^{(4)}_{ob}\right) + \underbrace{(1 - m\varepsilon_m)}_{1+\beta^2}\left(U^{(4)}_{ob} + U^{(2)}_{ob}\right) + \underbrace{-m\varepsilon_m}_{\beta^2}\left(U^{(2)}_{ob} + U_{ob}\right) = 0 \quad 1 - m\varepsilon_m = \chi^2\,,\ \ \beta^2 = -m\varepsilon_m \tag{71}$$

The differential equation (71) is associated with homogeneous boundary conditions, which together define an eigenvalue problem with ε_m as the eigenvalue. This eigenvalue problem can be solved either semi-analytically taking into account that

$$U_{ob} = \mathcal{E}_1 \cos\varphi + \mathcal{E}_2 \sin\varphi + \mathcal{E}_3 \left(\frac{1}{2}\varphi \sin\varphi + \cos\varphi\right) - \mathcal{E}_4 \left(\frac{1}{2}\varphi \cos\varphi - \sin\varphi\right) + \frac{\mathcal{E}_5}{1-\beta^2} \cos\beta\varphi + \frac{\mathcal{E}_6}{1-\beta^2} \sin\beta\varphi \tag{72}$$

(the undetermined integration constants are denoted by $\mathcal{E}_i,\ i = 1, \ldots, 6$) or numerically by following the procedure applied in the paper by Burmeister (2013) for the stability investigations of shell-stiffened circular plates. With the knowledge of the eigenvalue $\varepsilon_m = \varepsilon_m(\vartheta)$ the critical load can be computed from equation (46).
(ii) One can also assume that the rotation of the cross-sections is finite. This affects the kinematic hypotheses. Under this assumption one can also set up either a linearized model or a quadratic one for the buckling phenomenon.

Acknowledgements by the first author: This research was supported by the **European Union** and the **State of Hungary, co-financed by the European Social Fund** in the framework of TÁMOP 4.2.4.A/2-11-1-2012-0001 'National Excellence Program'.

The authors would like to thank the unknown reviewers for their constructive and helpful suggestions.

A.1 Detailed Manipulations

A.1.1 Formula for the Axial Force

Making use of the kinematic relations (8) and inequality (12) we can transform equation (10) into the form

$$\begin{aligned} N = A_e \underbrace{\left(\frac{\mathrm{d}u_o}{\mathrm{d}s} + \frac{w_o}{\rho_o} + \frac{1}{2}\psi_{o\eta}^2\right)}_{\varepsilon_m} + \frac{I_{e\eta}}{\rho_o} \frac{\mathrm{d}}{\mathrm{d}s}\left(\frac{\mathrm{d}w_o}{\mathrm{d}s} - \frac{u_o}{\rho_o}\right) = \\ = \frac{I_{e\eta}}{\rho_o^3}\left[\left(\frac{A_e\rho_o^2}{I_{e\eta}} - 1\right)\left(u_o^{(1)} + w_o\right) + w_o^{(2)} + w_o\right] + \frac{1}{2}\psi_{o\eta}^2 \underbrace{\left(\frac{A_e\rho_o^2}{I_{e\eta}} - 1 + 1\right)}_{\approx A_e\rho_o^2/I_{e\eta} - 1} \frac{I_{e\eta}}{\rho_o^2} = \\ = \frac{I_{e\eta}}{\rho_o^2}\left(\frac{A_e\rho_o^2}{I_{e\eta}} - 1\right) \underbrace{\left(\frac{1}{\rho_o}\left(u_o^{(1)} + w_o\right) + \frac{1}{2}\psi_{o\eta}^2\right)}_{\varepsilon_m} + \underbrace{\frac{I_{e\eta}}{\rho_o^3}\left(w_o^{(2)} + w_o\right)}_{-M/\rho_o} = \\ = \frac{I_{e\eta}}{\rho_o^2}\left(\frac{A_e\rho_o^2}{I_{e\eta}} - 1\right)\varepsilon_m - \frac{M}{\rho_o} \approx A_e\varepsilon_m - \frac{M}{\rho_o}\,. \end{aligned} \tag{A.1}$$

A similar line of thought for the increment N_b – see equation (18) – results in

$$\begin{aligned} N_b = A_e\left(\varepsilon_{o\xi\,b} + \psi_{o\eta}\psi_{o\eta\,b} + \frac{1}{2}\psi_{o\eta\,b}^2\right) + \frac{I_{e\eta}}{\rho_o^3}\left(w_{ob}^{(2)} - u_{ob}^{(1)}\right) + \frac{I_{e\eta}}{\rho_o^3}w_{ob} - \frac{I_{e\eta}}{\rho_o^3}w_{ob} = \\ = \frac{I_{e\eta}}{\rho_o^2}\left[\left(\frac{A_e\rho_o^2}{I_{e\eta}} - 1\right)\varepsilon_{o\xi\,b} + \frac{A_e\rho_o^2}{I_{e\eta}}\left(\psi_{o\eta}\psi_{o\eta\,b} + \frac{1}{2}\psi_{o\eta\,b}^2\right)\right] + \frac{I_{e\eta}}{\rho_o^3}\left(w_{ob}^{(2)} + w_{ob}\right) \approx \\ \approx \frac{I_{e\eta}}{\rho_o^2}\left(\frac{A_e\rho_o^2}{I_{e\eta}} - 1\right)\left[\varepsilon_{o\xi\,b} + \left(\psi_{o\eta}\psi_{o\eta\,b} + \frac{1}{2}\psi_{o\eta\,b}^2\right)\right] + \frac{I_{e\eta}}{\rho_o^3}\left(w_{ob}^{(2)} + w_{ob}\right) = \frac{I_{e\eta}}{\rho_o^2}m\varepsilon_{mb} + \frac{I_{e\eta}}{\rho_o^3}\left(w_{ob}^{(2)} + w_{ob}\right)\,. \end{aligned} \tag{A.2}$$

A.1.2 Transformation of the Principle of Virtual Work – Pre-buckling State

Substituting the corresponding kinematical quantities from (3)-(8) into the principle of virtual work (22) and taking the relation

$$\mathrm{d}V = \left(1 + \frac{\zeta}{\rho_o}\right)\mathrm{d}s\,\mathrm{d}A \tag{A.3}$$

(which provides the infinitesimal volume element) into account the left side of the principle can be rewritten as

$$\int_V \sigma_\xi \delta\varepsilon_\xi \,\mathrm{d}V = \int_{\mathcal{L}}\int_A \left(1 + \frac{\zeta}{\rho_o}\right)\sigma_\xi \left[\frac{1}{1 + \frac{\zeta}{\rho_o}}\left(\frac{\mathrm{d}\delta u_o}{\mathrm{d}s} + \frac{\delta w_o}{\rho_o} + \zeta\frac{\mathrm{d}\delta\psi_{o\eta}}{\mathrm{d}s}\right) + \psi_{o\eta}\,\delta\psi_{o\eta}\right]\mathrm{d}A\,\mathrm{d}s =$$

$$= \int_{\mathcal{L}} \left\{ \int_A \sigma_\xi \mathrm{d}A \left(\frac{\mathrm{d}\delta u_o}{\mathrm{d}s} + \frac{\delta w_o}{\rho_o} \right) + \int_A \zeta \sigma_\xi \mathrm{d}A \frac{\mathrm{d}\delta\psi_{o\eta}}{\mathrm{d}s} + \int_A \left(1 + \frac{\zeta}{\rho_o} \right) \sigma_\xi \, \mathrm{d}A \psi_{o\eta} \left(\frac{\delta u_o}{\rho_o} - \frac{\mathrm{d}\delta w_o}{\mathrm{d}s} \right) \right\} \mathrm{d}s =$$

$$= \int_{\mathcal{L}} \left[N \left(\frac{\mathrm{d}\delta u_o}{\mathrm{d}s} + \frac{\delta w_o}{\rho_o} \right) + M \frac{\mathrm{d}\delta\psi_{o\eta}}{\mathrm{d}s} + \left(N + \frac{M}{\rho_o} \right) \psi_{o\eta} \left(\frac{\delta u_o}{\rho_o} - \frac{\mathrm{d}\delta w_o}{\mathrm{d}s} \right) \right] \mathrm{d}s, \quad \text{(A.4)}$$

where formulae (10)-(12) for the inner forces have also been utilized. Apply now the integration by parts theorem and make the result obtained equal to the right side of (22). After some rearrangement we get

$$- \int_{\mathcal{L}} \left(\frac{\mathrm{d}N}{\mathrm{d}s} + \frac{1}{\rho_o} \frac{\mathrm{d}M}{\mathrm{d}s} - \frac{1}{\rho_o} \left(N + \frac{M}{\rho_o} \right) \psi_{o\eta} + f_t \right) \delta u_o \mathrm{d}s - \int_{\mathcal{L}} \left(\frac{\mathrm{d}^2 M}{\mathrm{d}s^2} - \frac{N}{\rho_o} - \frac{\mathrm{d}}{\mathrm{d}s} \left(N + \frac{M}{\rho_o} \right) \psi_{o\eta} + f_n \right) \delta w_o \mathrm{d}s -$$

$$- \left[\frac{\mathrm{d}M}{\mathrm{d}s} - \left(N + \frac{M}{\rho_o} \right) \psi_{o\eta} \right] \delta w_o \Big|_{s(-\vartheta)} + \left[\frac{\mathrm{d}M}{\mathrm{d}s} - \left(N + \frac{M}{\rho_o} \right) \psi_{o\eta} \right] \delta w_o \Big|_{s(\vartheta)} +$$

$$+ \left\{ \left[\frac{\mathrm{d}M}{\mathrm{d}s} - \left(N + \frac{M}{\rho_o} \right) \psi_{o\eta} \right] \Big|_{s=+0} - \left[\frac{\mathrm{d}M}{\mathrm{d}s} - \left(N + \frac{M}{\rho_o} \right) \psi_{o\eta} \right] \Big|_{s=-0} - P_\zeta \right\} \delta w_o|_{s=0} +$$

$$- N \delta u_o|_{s(-\vartheta)} + N \delta u_o|_{s(\vartheta)} + (M + k_{\gamma r} \psi_{o\eta})|_{s(\vartheta)} \, \delta\psi_{o\eta}|_{s(\vartheta)} - (M - k_{\gamma \ell} \psi_{o\eta})|_{s(-\vartheta)} \, \delta\psi_{o\eta}|_{s(-\vartheta)} = 0 \, . \quad \text{(A.5)}$$

Observe that $[|_{s=-0}](|_{s=+0})$ denote the [left](right) side limit of the expression preceding the symbol $|$.

A.1.3 Transformation of the Principle of Virtual Work – Post-buckling State

First resolve the quantities denoted by an asterisk in (30) into two parts – we should apply the resolutions presented in the first paragraph of Subsection 2.2. Then take into account that the kinematical quantities in the pre-buckling state are known, consequently, there belong no virtual quantities to them. Recalling formulae $(15)_1$ and (16) for the virtual rotation and strain we can write

$$\delta\psi^*_{o\eta} = \delta\psi_{o\eta\, b} = \frac{\delta u_{ob}}{\rho_o} - \frac{\mathrm{d}\delta w_{ob}}{\mathrm{d}s} \quad \text{(A.6)}$$

and

$$\delta\varepsilon^*_\xi = \delta\left(\varepsilon_\xi + \varepsilon_{\xi\, b}\right) = \delta\varepsilon_{\xi\, b} = \underbrace{\frac{1}{1 + \frac{\zeta}{\rho_o}} \left(\delta\varepsilon_{o\xi\, b} + \zeta \delta\kappa_{o\, b} \right) + \psi_{o\eta} \delta\psi_{o\eta\, b}}_{\delta\varepsilon^L_{\xi\, b}} + \underbrace{\psi_{o\eta\, b} \delta\psi_{o\eta\, b}}_{\delta\varepsilon^N_{\xi\, b}} =$$

$$= \underbrace{\frac{1}{1 + \frac{\zeta}{\rho_o}} \left(\frac{\mathrm{d}\delta u_{o\, b}}{\mathrm{d}s} + \frac{\delta w_{o\, b}}{\rho_o} + \zeta \frac{\mathrm{d}\delta\psi_{o\eta\, b}}{\mathrm{d}s} \right) + \psi_{o\eta} \delta\psi_{o\eta\, b}}_{\delta\varepsilon^L_{\xi\, b}} + \underbrace{\psi_{o\eta\, b} \delta\psi_{o\eta\, b}}_{\delta\varepsilon^N_{\xi\, b}} \, . \quad \text{(A.7)}$$

On the basis of all that has been said we can rewrite the principle of virtual work (30) into the form

$$0 = - \int_V \sigma_\xi \delta\varepsilon^N_{\xi\, b} \mathrm{d}V - \int_V \sigma_{\xi\, b} \delta\varepsilon^L_{\xi\, b} \, \mathrm{d}V - \int_V \sigma_{\xi\, b} \delta\varepsilon^N_{\xi\, b} \, \mathrm{d}V - P_{\zeta\, b} \, \delta w_{o\, b}|_{s=0} + P_{\xi\, b} \, \delta u_{o\, b}|_{s=0} -$$

$$- \mathfrak{m} \ddot{w}_{ob} \delta w_{o\, b}|_{s=0} - \mathfrak{m} \ddot{u}_{ob} \delta u_{o\, b}|_{s=0} - k_{\gamma\, \ell} \psi_{o\eta\, b} \delta\psi_{o\eta\, b}|_{s(-\vartheta)} - k_{\gamma\, r} \psi_{o\eta\, b} \delta\psi_{o\eta\, b}|_{s(\vartheta)} + \int_{\mathcal{L}} \left(f_{nb} \delta w_{ob} + f_{tb} \delta u_{o\, b} \right) \mathrm{d}s \, . \quad \text{(A.8)}$$

Observe that the three integrals require further manipulations based on the integration by parts theorem as detailed in the sequel

$$\int_V \sigma_\xi \delta\varepsilon^N_{\xi\, b} \mathrm{d}V = \int_{\mathcal{L}} \int_A \left(1 + \frac{\zeta}{\rho_o} \right) \sigma_\xi \delta\varepsilon^N_{\xi\, b} \mathrm{d}A \, \mathrm{d}s = \int_{\mathcal{L}} \left(N + \frac{M}{\rho_o} \right) \psi_{o\eta\, b} \left(\frac{\delta u_{ob}}{\rho_o} - \frac{\mathrm{d}\delta w_{ob}}{\mathrm{d}s} \right) \mathrm{d}s =$$

$$= \int_{\mathcal{L}} \frac{1}{\rho_o} \left(N + \frac{M}{\rho_o} \right) \psi_{o\eta\, b} \delta u_{ob} \mathrm{d}s + \int_{\mathcal{L}} \left[\frac{\mathrm{d}}{\mathrm{d}s} \left(N + \frac{M}{\rho_o} \right) \psi_{o\eta\, b} \right] \delta w_{ob} \mathrm{d}s - \left(N + \frac{M}{\rho_o} \right) \psi_{o\eta\, b} \, \delta w_{ob}|_{s=0} +$$

$$+ \left(N + \frac{M}{\rho_o} \right) \psi_{o\eta\, b} \delta w_{ob} \Big|_{s(-\vartheta)} - \left(N + \frac{M}{\rho_o} \right) \psi_{o\eta\, b} \delta w_{ob} \Big|_{s(\vartheta)} \, . \quad \text{(A.9)}$$

Furthermore

$$\int_V \sigma_{\xi\, b} \delta\varepsilon^L_{\xi\, b} \, \mathrm{d}V = \int_{\mathcal{L}} \int_A \left(1 + \frac{\zeta}{\rho_o} \right) \sigma_{\xi\, b} \left[\frac{1}{1 + \frac{\zeta}{\rho_o}} \left(\frac{\mathrm{d}\delta u_{o\, b}}{\mathrm{d}s} + \frac{\delta w_{o\, b}}{\rho_o} + \zeta \frac{\mathrm{d}\delta\psi_{o\eta\, b}}{\mathrm{d}s} \right) + \psi_{o\eta} \delta\psi_{o\eta\, b} \right] \mathrm{d}A \, \mathrm{d}s =$$

$$= \int_{\mathcal{L}} \left\{ N_b \left(\frac{\mathrm{d}\delta u_{o\, b}}{\mathrm{d}s} + \frac{\delta w_{o\, b}}{\rho_o} \right) + M_b \frac{\mathrm{d}}{\mathrm{d}s} \left(\frac{\delta u_{ob}}{\rho_o} - \frac{\mathrm{d}\delta w_{ob}}{\mathrm{d}s} \right) + \left(N_b + \frac{M_b}{\rho_o} \right) \psi_{o\eta} \left(\frac{\delta u_{ob}}{\rho_o} - \frac{\mathrm{d}\delta w_{ob}}{\mathrm{d}s} \right) \right\} \mathrm{d}s =$$

$$= - \int_{\mathcal{L}} \frac{\mathrm{d}N_b}{\mathrm{d}s} \delta u_{o\, b} \mathrm{d}s - N_b \delta u_{o\, b}|_{s(-\vartheta)} + \left[N_b|_{s=-0} - N_b|_{s=+0} \right] \delta u_{o\, b}|_{s=0} + N_b \delta u_{o\, b}|_{s(\vartheta)} +$$

$$+\int_{\mathcal{L}}\frac{N_b}{\rho_o}\delta w_{o\,b}\,\mathrm{d}s-\int_{\mathcal{L}}\frac{1}{\rho_o}\frac{\mathrm{d}M_b}{\mathrm{d}s}\delta u_{ob}\mathrm{d}s-\int_{\mathcal{L}}\frac{\mathrm{d}^2M_b}{\mathrm{d}s^2}\delta w_{ob}\mathrm{d}s+M_b\delta\psi_{o\eta\,b}|_{s(\vartheta)}-M_b\delta\psi_{o\eta\,b}|_{s(-\vartheta)}-$$
$$-\frac{\mathrm{d}M_b}{\mathrm{d}s}\delta w_{ob}\Big|_{s(-\vartheta)}+\left[\frac{\mathrm{d}M_b}{\mathrm{d}s}\Big|_{s=-0}-\frac{\mathrm{d}M_b}{\mathrm{d}s}\Big|_{s=+0}\right]\delta w_{ob}|_{s=0}+\frac{\mathrm{d}M_b}{\mathrm{d}s}\delta w_{ob}\Big|_{s(\vartheta)}+$$
$$+\int_{\mathcal{L}}\frac{1}{\rho_o}\frac{\mathrm{d}}{\mathrm{d}s}\left(N_b+\frac{M_b}{\rho_o}\right)\psi_{o\eta}\delta u_{ob}\mathrm{d}s+\int_{\mathcal{L}}\left[\frac{\mathrm{d}}{\mathrm{d}s}\left(N_b+\frac{M_b}{\rho_o}\right)\psi_{o\eta}\right]\delta w_{ob}\mathrm{d}s-\left(N_b+\frac{M_b}{\rho_o}\right)\psi_{o\eta}\delta w_{ob}\Big|_{s(-\vartheta)}^{s(\vartheta)}\,. \quad (A.10)$$

The third integral is formally the same as the first one if we change σ_ξ to $\sigma_{\xi\,b}$, therefore

$$\int_V\sigma_\xi\delta\varepsilon^N_{\xi\,b}\mathrm{d}V=\int_{\mathcal{L}}\int_A\left(1+\frac{\zeta}{\rho_o}\right)\sigma_{\xi b}\delta\varepsilon^N_{\xi\,b}\mathrm{d}A\,\mathrm{d}s=\int_{\mathcal{L}}\left(N_b+\frac{M_b}{\rho_o}\right)\psi_{o\eta\,b}\left(\frac{\delta u_{ob}}{\rho_o}-\frac{\mathrm{d}\delta w_{ob}}{\mathrm{d}s}\right)\mathrm{d}s=$$
$$=\int_{\mathcal{L}}\frac{1}{\rho_o}\left(N_b+\frac{M_b}{\rho_o}\right)\psi_{o\eta\,b}\delta u_{ob}\mathrm{d}s+\int_{\mathcal{L}}\left[\frac{\mathrm{d}}{\mathrm{d}s}\left(N_b+\frac{M_b}{\rho_o}\right)\psi_{o\eta\,b}\right]\delta w_{ob}\mathrm{d}s-\left(N_b+\frac{M_b}{\rho_o}\right)\psi_{o\eta\,b}\;\delta w_{ob}|_{s=0}+$$
$$+\left(N_b+\frac{M_b}{\rho_o}\right)\psi_{o\eta\,b}\delta w_{ob}\Big|_{s(-\vartheta)}-\left(N_b+\frac{M_b}{\rho_o}\right)\psi_{o\eta\,b}\delta w_{ob}\Big|_{s(\vartheta)}\,. \quad (A.11)$$

As a summary of these manipulations the principle of virtual work that is equation (30) can be rewritten in a final form as

$$-\int_{\mathcal{L}}\left(\frac{\mathrm{d}N_b}{\mathrm{d}s}-\frac{1}{\rho_o}\left(N+\frac{M}{\rho_o}\right)\psi_{o\eta\,b}+\frac{1}{\rho_o}\left[\frac{\mathrm{d}M_b}{\mathrm{d}s}-\left(N_b+\frac{M_b}{\rho_o}\right)\psi_{o\eta\,b}\right]+f_{tb}\right)\delta u_{o\,b}\mathrm{d}s-$$
$$-\int_{\mathcal{L}}\left(\frac{\mathrm{d}^2M_b}{\mathrm{d}s^2}-\frac{N_b}{\rho_o}-\frac{\mathrm{d}}{\mathrm{d}s}\left[\left(N+N_b+\frac{M+M_b}{\rho_o}\right)\psi_{o\eta\,b}+\left(N_b+\frac{M_b}{\rho_o}\right)\psi_{o\eta}\right]+f_{nb}\right)\delta w_{ob}\mathrm{d}s-$$
$$-\left[\frac{\mathrm{d}M_b}{\mathrm{d}s}-\left(N+N_b+\frac{M+M_b}{\rho_o}\right)\psi_{o\eta\,b}-\left(N_b+\frac{M_b}{\rho_o}\right)\psi_{o\eta}\right]\delta w_{ob}\Big|_{s(-\vartheta)}+$$
$$+\left[\frac{\mathrm{d}M_b}{\mathrm{d}s}-\left(N+N_b+\frac{M+M_b}{\rho_o}\right)\psi_{o\eta\,b}-\left(N_b+\frac{M_b}{\rho_o}\right)\psi_{o\eta}\right]\delta w_{ob}\Big|_{s(\vartheta)}+$$
$$+\left\{\left[\frac{\mathrm{d}M_b}{\mathrm{d}s}-\left(N+N_b+\frac{M+M_b}{\rho_o}\right)\psi_{o\eta\,b}-\left(N_b+\frac{M_b}{\rho_o}\right)\psi_{o\eta}\right]\Big|_{s=-0}-\right.$$
$$\left.-\left[\frac{\mathrm{d}M_b}{\mathrm{d}s}-\left(N+N_b+\frac{M+M_b}{\rho_o}\right)\psi_{o\eta\,b}-\left(N_b+\frac{M_b}{\rho_o}\right)\psi_{o\eta}\right]\Big|_{s=+0}+\mathfrak{m}\;\frac{\mathrm{d}^2w}{\mathrm{d}t^2}\Big|_{s=0}\right\}\delta w_{ob}|_{s=0}-$$
$$-N_b\delta u_{o\,b}|_{s(-\vartheta)}+\left[N_b|_{s=-0}-N_b|_{s=+0}+P_{\xi\,b}+\mathfrak{m}\;\frac{\mathrm{d}^2u}{\mathrm{d}t^2}\Big|_{s=0}\right]\delta u_{o\,b}|_{s=0}+N_b\delta u_{o\,b}|_{s(\vartheta)}+$$
$$+(M_b+k_{\gamma\,r}\psi_{o\eta\,b})|_\vartheta\;\delta\psi_{o\eta\,b}|_{s(\vartheta)}-(M_b-k_{\gamma\,\ell}\psi_{o\eta\,b})|_{s(-\vartheta)}\;\delta\psi_{o\eta\,b}|_{s(-\vartheta)}=0\,. \quad (A.12)$$

A.1.4 Pre-buckling Equilibrium in Terms of the Displacements

It follows from equation $(23)_2$ that

$$\frac{\mathrm{d}^2M}{\mathrm{d}s^2}-\psi_{o\eta}\frac{\mathrm{d}}{\mathrm{d}s}\left(N+\frac{M}{\rho_o}\right)-\left(N+\frac{M}{\rho_o}\right)\frac{\mathrm{d}\psi_{o\eta}}{\mathrm{d}s}-\frac{N}{\rho_o}=0\,.$$

Substitute here now equations (12) and (14), which give the inner forces in terms of the displacements. The first and third terms require no further manipulations at this point. The second one, however, vanishes – compare (14) and (27). As for the fourth one some transformations need to be carried out as detailed here:

$$\frac{N}{\rho_o}=\frac{A_e}{\rho_o}\varepsilon_m-\frac{M}{\rho_o^2}=\frac{I_{e\eta}}{\rho_o^3}\frac{A_e\rho_o^2}{I_{e\eta}}\varepsilon_m-\frac{M}{\rho_o^2}=\frac{I_{e\eta}}{\rho_o^3}m\varepsilon_m+\frac{I_{e\eta}}{\rho_o^4}\left(w_o^{(2)}+w_o\right)\,.$$

Consequently, the equilibrium condition can now be rewritten as

$$-\frac{I_{e\eta}}{\rho_o^4}\left(w_o^{(4)}+w_o^{(2)}\right)-\frac{I_{e\eta}}{\rho_o^4}\frac{A_e\rho_o^2}{I_{e\eta}}\rho_o\varepsilon_m\psi_{o\eta}^{(1)}-\frac{I_{e\eta}}{\rho_o^3}m\varepsilon_m-\frac{I_{e\eta}}{\rho_o^4}\left(w_o^{(2)}+w_o\right)=0\,.$$

Multiplying this formula with $-\rho_o^4/I_{e\eta}$ we have

$$\left(w_o^{(4)}+w_o^{(2)}\right)+\rho_om\varepsilon_m\left(\psi_{o\eta}^{(1)}+1\right)+\left(w_o^{(2)}+w_o\right)=0\,. \quad (A.13)$$

If we substitute $\psi_{o\eta}$ from (3) and $u_o^{(1)}$ from $(8)_1$ into the expression $\rho_o\varepsilon_m\left(1+\psi_{o\eta}^{(1)}\right)$ and utilize $(8)_3$ then we arrive at the following result (the quadratic term is neglected when that is compared to the others):

$$\rho_o\varepsilon_m\left(1+\psi_{o\eta}^{(1)}\right)=\rho_o\varepsilon_m\left[1+\frac{1}{\rho_o}\left(u_o^{(1)}-w_o^{(2)}\right)\right]=\rho_o\varepsilon_m\left[1+\frac{1}{\rho_o}\left(\rho_o\varepsilon_m-w_o-\frac{1}{2}\psi_{o\eta}^2\rho_o-w_o^{(2)}\right)\right]\approx$$
$$\approx\rho_o\varepsilon_m\underbrace{(1+\varepsilon_m)}_{\approx 1}-\varepsilon_m\left(w_o+w_o^{(2)}\right)\approx\rho_o\varepsilon_m-\varepsilon_m\left(w_o^{(2)}+w_o\right)\,. \quad \text{(A.14)}$$

Upon substitution of the above equation into (A.13) we have that the pre-buckling displacement w_o should satisfy the differential equation

$$w_o^{(4)}+2w_o^{(2)}+w_o-m\varepsilon_m\left(w_o^{(2)}+w_o\right)=-m\rho_o\varepsilon_m\,. \quad \text{(A.15)}$$

A.1.5 Post-buckling Equilibrium in Terms of Displacements

We shall assume that $f_{nb}=0$. It follows from a comparison of equations (14) and (27) as well as (21) and (34) that

$$\frac{\mathrm{d}}{\mathrm{d}s}\left(N+\frac{M}{\rho_o}\right)=0\,,\qquad \frac{\mathrm{d}}{\mathrm{d}s}\left(N_b+\frac{M_b}{\rho_o}\right)=0\,.$$

Consequently, equation (31b) assumes the form

$$-\frac{\mathrm{d}^2M_b}{\mathrm{d}s^2}+\frac{N_b}{\rho_o}+\underbrace{\left(N+\frac{M}{\rho_o}\right)}_{A_e\varepsilon_m}\frac{\mathrm{d}\psi_{o\eta\,b}}{\mathrm{d}s}+\underbrace{\left(N_b+\frac{M_b}{\rho_o}\right)}_{A_e\varepsilon_{mb}}\frac{\mathrm{d}\psi_{o\eta}}{\mathrm{d}s}=0, \quad \text{(A.16)}$$

where we have neglected the terms quadratic in the increments. As regards the last two terms some transformations with the aid of (12), (14) and (21) need to be carried out

$$A_e\varepsilon_m\frac{\mathrm{d}\psi_{o\eta\,b}}{\mathrm{d}s}+A_e\varepsilon_{mb}\frac{\mathrm{d}\psi_{o\eta}}{\mathrm{d}s}=m\frac{I_{e\eta}}{\rho_o^2}\left(\varepsilon_m\frac{\mathrm{d}\psi_{o\eta\,b}}{\mathrm{d}s}+\varepsilon_{mb}\frac{\mathrm{d}\psi_{o\eta}}{\mathrm{d}s}\right)\,. \quad \text{(A.17)}$$

Substitute now M_b from (20), N_b from (21) (utilizing again (20)) into (A.16) and take equation (12) into account. In this way we have

$$\frac{I_{e\eta}}{\rho_o^4}\left(w_{ob}^{(4)}+w_{ob}^{(2)}\right)+\frac{I_{e\eta}}{\rho_o^4}\left(w_{ob}^{(2)}+w_{ob}\right)+m\frac{I_{e\eta}}{\rho_o^3}\varepsilon_{mb}+m\frac{I_{e\eta}}{\rho_o^3}\varepsilon_m\psi_{o\eta\,b}^{(1)}+m\frac{I_{e\eta}}{\rho_o^3}\varepsilon_{mb}\psi_{o\eta}^{(1)}=0\,. \quad \text{(A.18)}$$

Let us multiply the former expression by $\rho_o^4/I_{e\eta}$. After some minor arrangements we obtain

$$w_{ob}^{(4)}+2w_{ob}^{(2)}+w_{ob}+m\rho_o\varepsilon_{mb}\left(1+\psi_{o\eta}^{(1)}\right)+m\rho_o\varepsilon_m\psi_{o\eta\,b}^{(1)}=0\,. \quad \text{(A.19)}$$

Now repeating the line of thought leading to (A.14) – but now by formally changing ε_m to ε_{mb} – we can write that

$$m\rho_o\varepsilon_{mb}\left(1+\psi_{o\eta}^{(1)}\right)\simeq m\rho_o\varepsilon_{mb}\left[1-\frac{1}{\rho_o}\left(w_o^{(2)}+w_o\right)\right]=m\rho_o\varepsilon_{mb}-m\varepsilon_{mb}\left(w_o^{(2)}+w_o\right)\,.$$

In a similar way (with the omission of the unit) the previous procedure can be applied as well to the last term in (A.19)

$$m\rho_o\varepsilon_m\psi_{o\eta\,b}^{(1)}\simeq-m\varepsilon_m\left(w_{ob}^{(2)}+w_{ob}\right)\,.$$

Altogether

$$w_{ob}^{(4)}+(2-m\varepsilon_m)\,w_{ob}^{(2)}+(1-m\varepsilon_m)\,w_{ob}=-m\rho_o\varepsilon_{mb}-m\varepsilon_{mb}\left(w_o^{(2)}+w_o\right), \quad \text{(A.20)}$$

which is the post-buckling equilibrium equation in terms of the displacements.

A.1.6 Calculation of the Pre-buckling Strain

For a pinned-pinned beam substitution of $W_{o\,r}$ from (41) into (43) results in

$$\varepsilon_{o\xi}=\frac{1}{\vartheta}\int_0^{\vartheta}W_{o\,r}\,\mathrm{d}\varphi=\frac{1}{\vartheta}\left[\int_0^{\vartheta}\left(\frac{\chi^2-1}{\chi^2}+A_{11}\cos\varphi-\frac{A_{31}}{\chi^2}\cos\chi\varphi\right)\mathrm{d}\varphi+\right.$$
$$\left.+\int_0^{\vartheta}\left(A_{12}\cos\varphi+A_{22}\sin\varphi-\frac{A_{32}}{\chi^2}\cos\chi\varphi-\frac{A_{42}}{\chi^2}\sin\chi\varphi\right)\right]\mathrm{d}\varphi\frac{\mathcal{P}}{\vartheta}=I_{ow}+I_{1w}\frac{\mathcal{P}}{\vartheta},$$

where

$$I_{ow}=1-\frac{1}{\chi^2}-\frac{\tan\vartheta}{\vartheta}+\frac{\tan\chi\vartheta}{\chi^3\vartheta}\,,\qquad I_{1w}=\frac{1}{\vartheta\,(\chi^2-1)}\left(1\,-\frac{1}{\chi^2}-\frac{1}{\cos\vartheta}+\frac{1}{\chi^2\cos\chi\vartheta}\right)\,. \quad \text{(A.21)}$$

Consequently,

$$I_{ow}=\frac{\chi^2-1}{\chi^2}-\frac{(\chi-1)^2\,(\chi+1)^2}{\chi^3\vartheta}\frac{\sin\vartheta\sin\chi\vartheta}{\mathcal{D}}\,,\qquad I_{1w}=\frac{1}{\vartheta\chi^2}\frac{\chi\,(\cos\vartheta-1)\sin\chi\vartheta+(1-\cos\chi\vartheta)\sin\vartheta}{\mathcal{D}}\,. \quad \text{(A.22)}$$

To calculate the nonlinear strain we need to know the square of the rotation. Recalling equation (42) we have

$$\psi_{o\eta}^2 \simeq \left[D_{11}\sin\varphi + D_{31}\sin\chi\varphi + \left(D_{12}\sin\varphi + D_{22}\cos\varphi + D_{32}\sin\chi\varphi + D_{42}\cos\chi\varphi\right)\frac{\mathcal{P}}{\vartheta}\right]^2 =$$
$$= \left(D_{11}\sin\varphi + D_{31}\sin\chi\varphi\right)^2 + 2\left(D_{11}\sin\varphi + D_{31}\sin\chi\varphi\right)\left(D_{12}\sin\varphi + D_{22}\cos\varphi + D_{32}\sin\chi\varphi + D_{42}\cos\chi\varphi\right)\frac{\mathcal{P}}{\vartheta} +$$
$$+ \left(D_{12}\sin\varphi + D_{22}\cos\varphi + D_{32}\sin\chi\varphi + D_{42}\cos\chi\varphi\right)^2\left(\frac{\mathcal{P}}{\vartheta}\right)^2 . \quad \text{(A.23)}$$

Accordingly, we can now calculate the missing terms in (45). These are sought in the form

$$\frac{1}{\vartheta}\int_0^{\vartheta}\frac{1}{2}\psi_{o\eta}^2(\varphi)\,\mathrm{d}\varphi = I_{0\psi} + I_{1\psi}\frac{\mathcal{P}}{\vartheta} + I_{2\psi}\left(\frac{\mathcal{P}}{\vartheta}\right)^2 . \quad \text{(A.24)}$$

Here

$$I_{0\psi} = \frac{1}{2\vartheta}\int_0^{\vartheta}\left(D_{11}(\sin\varphi) + D_{31}(\sin\chi\varphi)\right)^2\mathrm{d}\varphi = \frac{-1}{8\vartheta\chi\left(1-\chi^2\right)}\times$$
$$\times\left\{D_{11}^2\chi\left(\sin 2\vartheta - 2\vartheta\right) + \frac{8D_{11}D_{31}\chi\left[\left(\sin\chi\vartheta\right)\cos\vartheta - \chi\left(\cos\chi\vartheta\right)\sin\vartheta\right]}{\left(1-\chi^2\right)} + D_{31}^2\left(\left(\sin 2\chi\vartheta\right) - 2\vartheta\chi\right)\right\} . \quad \text{(A.25)}$$

To simplify the evaluation it is advisable to decompose $I_{1\psi}$:

$$I_{1\psi} = \frac{1}{\vartheta}\int_0^{\vartheta}\left(D_{11}\sin\varphi + D_{31}\sin\chi\varphi\right)\left(D_{12}\sin\varphi + D_{22}\cos\varphi + D_{32}\sin\chi\varphi + D_{42}\cos\chi\varphi\right)\,\mathrm{d}\varphi =$$
$$= \underbrace{\frac{1}{\vartheta}\int_0^{\vartheta}D_{11}(\sin\varphi)\left(D_{12}\sin\varphi + D_{22}\cos\varphi + D_{32}\sin\chi\varphi + D_{42}\cos\chi\varphi\right)\,\mathrm{d}\varphi}_{I_{1\psi A}} +$$
$$+ \underbrace{\frac{1}{\vartheta}\int_0^{\vartheta}D_{31}(\sin\chi\varphi)\left(D_{12}\sin\varphi + D_{22}\cos\varphi + D_{32}\sin\chi\varphi + D_{42}\cos\chi\varphi\right)\,\mathrm{d}\varphi}_{I_{1\psi B}} = I_{1\psi A} + I_{1\psi B} . \quad \text{(A.26)}$$

The first part of the integral $I_{1\psi}$ can be written in the form

$$I_{1\psi A} = \frac{-D_{11}}{4\vartheta\left(1-\chi^2\right)}\left\{D_{12}\left(1-\chi^2\right)\left(\sin 2\vartheta - 2\vartheta\right) + D_{22}\left(1-\chi^2\right)\left(\cos 2\vartheta - 1\right) +\right.$$
$$\left. + 4D_{32}\left[\left(\sin\chi\vartheta\right)\cos\vartheta - \chi\left(\cos\chi\vartheta\right)\sin\vartheta\right] + 4D_{42}\left[\left(\cos\chi\vartheta\right)\cos\vartheta + \chi\left(\sin\chi\vartheta\right)\sin\vartheta - 1\right]\right\} . \quad \text{(A.27a)}$$

As regards the second part of the integral $I_{1\psi}$ we have

$$I_{1\psi B} = \frac{D_{31}}{4\chi\vartheta\left(1-\chi^2\right)}\left\{4\chi D_{12}\left[\chi\left(\cos\chi\vartheta\right)\sin\vartheta - \left(\sin\chi\vartheta\right)\cos\vartheta\right] + 4\chi D_{22}\left[\left(\sin\chi\vartheta\right)\sin\vartheta + \chi\left(\cos\chi\vartheta\right)\cos\vartheta - \chi\right] +\right.$$
$$\left. + D_{32}\left(1-\chi^2\right)\left[2\vartheta\chi - \left(\sin 2\chi\vartheta\right)\right] + D_{42}\left(1-\chi^2\right)\left[1 - \left(\cos 2\chi\vartheta\right)\right]\right\} . \quad \text{(A.27b)}$$

Moving on now to the calculation of $I_{2\psi}$ in (A.24) it is again worth decomposing the factor in question but for this time into four parts

$$I_{2\psi} = \frac{1}{2\vartheta}\int_0^{\vartheta}\left(D_{12}\sin\varphi + D_{22}\cos\varphi + D_{32}\sin\chi\varphi + D_{42}\cos\chi\varphi\right)^2\,\mathrm{d}\varphi =$$
$$= \underbrace{\frac{1}{\vartheta}\int_0^{\vartheta}\left(D_{12}\sin\varphi + D_{22}\cos\varphi + D_{32}\sin\chi\varphi + D_{42}\cos\chi\varphi\right)\,D_{12}(\sin\varphi)\,\mathrm{d}\varphi}_{I_{2\psi A}} +$$
$$+ \underbrace{\frac{1}{2\vartheta}\int_0^{\vartheta}\left(D_{12}\sin\varphi + D_{22}\cos\varphi + D_{32}\sin\chi\varphi + D_{42}\cos\chi\varphi\right)D_{22}(\cos\varphi)\,\mathrm{d}\varphi}_{I_{2\psi B}} +$$
$$+ \underbrace{\frac{1}{2\vartheta}\int_0^{\vartheta}\left(D_{12}\sin\varphi + D_{22}\cos\varphi + D_{32}\sin\chi\varphi + D_{42}\cos\chi\varphi\right)D_{32}(\sin\chi\varphi)\,\mathrm{d}\varphi}_{I_{2\psi C}} +$$
$$+ \underbrace{\frac{1}{2\vartheta}\int_0^{\vartheta}\left(D_{12}\sin\varphi + D_{22}\cos\varphi + D_{32}\sin\chi\varphi + D_{42}\cos\chi\varphi\right)D_{42}(\cos\chi\varphi)\,\mathrm{d}\varphi}_{I_{2\psi D}} =$$

$$= I_{2\psi A} + I_{2\psi B} + I_{2\psi C} + I_{2\psi D} \ . \quad \text{(A.28)}$$

The first term in this sum is

$$I_{2\psi A} = \frac{D_{12}}{8\vartheta\left(1-\chi^2\right)}\left\{D_{12}\left(1-\chi^2\right)\left[2\vartheta-\sin 2\vartheta\right]+D_{22}\left(1-\chi^2\right)\left[1-\cos 2\vartheta\right]+\right.$$
$$\left.+\,4D_{32}\left(\chi\left(\cos\chi\vartheta\right)\sin\vartheta-\left(\sin\chi\vartheta\right)\cos\vartheta\right)+4D_{42}\left[1-\left(\cos\chi\vartheta\right)\cos\vartheta-\chi\left(\sin\chi\vartheta\right)\sin\vartheta\right]\right\} \ . \quad \text{(A.29a)}$$

The second one can be expressed as

$$I_{2\psi B} = \frac{-D_{22}}{8\vartheta\left(\chi^2-1\right)}\left\{D_{12}\left(\chi^2-1\right)\left(\cos 2\vartheta-1\right)-D_{22}\left(\chi^2-1\right)\left(\sin 2\vartheta+2\vartheta\right)+\right.$$
$$\left.+\,4D_{32}\left[\chi\left(\cos\chi\vartheta\right)\cos\vartheta+\left(\sin\chi\vartheta\right)\sin\vartheta-\chi\right]+4D_{42}\left[\left(\cos\chi\vartheta\right)\sin\vartheta-\chi\left(\sin\chi\vartheta\right)\cos\vartheta\right]\right\} \ . \quad \text{(A.29b)}$$

Moreover, for the third part, the integration yields

$$I_{2\psi C} = \frac{D_{32}}{8\chi\vartheta\left(1-\chi^2\right)}\left\{4D_{12}\chi\left[\chi\left(\cos\chi\vartheta\right)\sin\vartheta-\left(\sin\chi\vartheta\right)\cos\vartheta\right]+4D_{22}\chi\left[\left(\sin\chi\vartheta\right)\sin\vartheta+\chi\left(\cos\chi\vartheta\right)\cos\vartheta-\chi\right]+\right.$$
$$\left.+D_{32}\left(1-\chi^2\right)\left[2\vartheta\chi-\sin 2\chi\vartheta\right]+D_{42}\left(1-\chi^2\right)\left[1-\cos 2\chi\vartheta\right]\right\} \quad \text{(A.29c)}$$

and finally, for the the last one we have

$$I_{2\psi D} = \frac{D_{42}}{8\vartheta\chi\left(\chi^2-1\right)}\left\{4D_{12}\chi\left[\left(\cos\chi\vartheta\right)\cos\vartheta+\chi\left(\sin\chi\vartheta\right)\sin\vartheta-1\right]+4D_{22}\chi\left[\chi\left(\sin\chi\vartheta\right)\cos\vartheta-\left(\cos\chi\vartheta\right)\sin\vartheta\right]\right.$$
$$\left.+\,2D_{32}\left(\chi^2-1\right)\sin^2\chi\vartheta+\,2D_{42}\left(\chi^2-1\right)\left[\chi\vartheta+\left(\sin\chi\vartheta\right)\cos\chi\vartheta\right]\right\} \ . \quad \text{(A.29d)}$$

A.1.7 Manipulations on the Displacement Increment

The solution to equation system (56) is as follows:

$$C_1 = -m\varepsilon_{mb}\frac{-A_3\cos\chi\vartheta+A_4\left(\chi\sin\vartheta-\sin\chi\vartheta\right)-1}{\chi^2\left(\chi^2-1\right)\cos\vartheta} \ , \quad \text{(A.30a)}$$

$$C_2 = m\varepsilon_{mb}\frac{A_4}{\chi\left(\chi^2-1\right)} \ , \qquad C_3 = -m\varepsilon_{mb}\frac{\left(3\chi^2-1\right)A_4}{2\chi^4\left(\chi^2-1\right)} \ , \quad \text{(A.30b)}$$

$$C_4 = -m\varepsilon_{mb}\frac{\chi\left[\vartheta\left(1-\chi^2\right)\sin\chi\vartheta+2\chi\cos\chi\vartheta\right]A_3+\left(1-\chi^2\right)\left[\sin\chi\vartheta-\vartheta\chi\cos\chi\vartheta\right]A_4+2}{2\chi^4\left(\chi^2-1\right)\cos\chi\vartheta} \ . \quad \text{(A.30c)}$$

It is advisable to decompose each of these into two parts: one in relation with the loading and the other not. Recalling and substituting here A_3 and A_4 from (39) we obtain after some arrangements that

$$C_1 = \varepsilon_{mb}\left(m\frac{A_{31}\cos\chi\vartheta+1}{\left(\chi^2-1\right)\chi^2\cos\vartheta}+m\frac{A_{32}\cos\chi\vartheta-A_{42}\left(\chi\sin\vartheta-\sin\chi\vartheta\right)}{\left(\chi^2-1\right)\chi^2\cos\vartheta}\frac{\mathcal{P}}{\vartheta}\right)=\varepsilon_{mb}\left(\hat{C}_{11}+\hat{C}_{12}\frac{\mathcal{P}}{\vartheta}\right) \ , \quad \text{(A.31a)}$$

$$C_2 = \varepsilon_{mb}m\frac{A_{42}}{\left(\chi^2-1\right)\chi}\frac{\mathcal{P}}{\vartheta}=\varepsilon_{mb}\hat{C}_{22}\frac{\mathcal{P}}{\vartheta} \ , \qquad C_3 = \varepsilon_{mb}m\frac{\left(1-3\chi^2\right)A_{42}}{2\chi^4\left(\chi^2-1\right)}\frac{\mathcal{P}}{\vartheta}=\varepsilon_{mb}\hat{C}_{32}\frac{\mathcal{P}}{\vartheta} \ , \quad \text{(A.31b)}$$

$$C_4 = \varepsilon_{mb}m\frac{2+A_{31}\left[\chi\vartheta\left(1-\chi^2\right)\sin\chi\vartheta+2\chi^2\cos\chi\vartheta\right]}{2\chi^4\left(1-\chi^2\right)\cos\chi\vartheta}+$$
$$+\,\varepsilon_{mb}m\frac{\mathcal{P}}{\vartheta}\frac{A_{32}\left[\chi\vartheta\left(1-\chi^2\right)\sin\chi\vartheta+2\chi^2\cos\chi\vartheta\right]+A_{42}\left(\chi^2-1\right)\left(\chi\vartheta\cos\chi\vartheta-\sin\chi\vartheta\right)}{2\chi^4\left(1-\chi^2\right)\cos\chi\vartheta}=\varepsilon_{mb}\left(\hat{C}_{41}+\hat{C}_{42}\frac{\mathcal{P}}{\vartheta}\right) \quad \text{(A.31c)}$$

with new constants defined by

$$\hat{C}_{11} = m\frac{A_{31}\cos\chi\vartheta+1}{\chi^2\left(\chi^2-1\right)\cos\vartheta} \ , \qquad \hat{C}_{12} = m\frac{A_{32}\cos\chi\vartheta-A_{42}\left(\chi\sin\vartheta-\sin\chi\vartheta\right)}{\chi^2\left(\chi^2-1\right)\cos\vartheta} \ , \quad \text{(A.32a)}$$

$$\hat{C}_{22} = m\frac{A_{42}}{\chi\left(\chi^2-1\right)} \ , \qquad \hat{C}_{32} = m\frac{\left(1-3\chi^2\right)A_{42}}{2\chi^4\left(\chi^2-1\right)} \ , \quad \text{(A.32b)}$$

$$\hat{C}_{41} = m\frac{2+A_{31}\chi\left[\vartheta\left(1-\chi^2\right)\sin\chi\vartheta+2\chi\cos\chi\vartheta\right]}{2\chi^4\left(1-\chi^2\right)\cos\chi\vartheta} \ , \quad \text{(A.32c)}$$

$$\hat{C}_{42} = m\frac{A_{32}\chi\left[\vartheta\left(1-\chi^2\right)\sin\chi\vartheta+2\chi\cos\chi\vartheta\right]+A_{42}\left(\chi^2-1\right)\left(\chi\vartheta\cos\chi\vartheta-\sin\chi\vartheta\right)}{2\chi^4\left(1-\chi^2\right)\cos\chi\vartheta} \ . \quad \text{(A.32d)}$$

In order to be able to rewrite the solution W_{ob} in a desired form the particular solution in (50) should be manipulated into the following form

$$
\begin{aligned}
-\varepsilon_{mb}\frac{m}{2\chi^3}\left(\frac{2}{\chi}+A_3\varphi\sin\chi\varphi-A_4\varphi\cos\chi\varphi\right) = \\
= -\varepsilon_{mb}\frac{m}{2\chi^3}\frac{2}{\chi}-\varepsilon_{mb}\frac{m}{2\chi^3}\left(A_{31}+A_{32}\frac{\mathcal{P}}{\vartheta}\right)\varphi\sin\chi\varphi+\varepsilon_{mb}\frac{m}{2\chi^3}\left(A_{42}\frac{\mathcal{P}}{\vartheta}\right)\varphi\cos\chi\varphi = \\
= \varepsilon_{mb}\left[-\frac{m}{\chi^4}-\frac{A_{31}m}{2\chi^3}\varphi\sin\chi\varphi+\left(-\frac{A_{32}m}{2\chi^3}\varphi\sin\chi\varphi+\frac{A_{42}m}{2\chi^3}\varphi\cos\chi\varphi\right)\frac{\mathcal{P}}{\vartheta}\right] = \\
= \varepsilon_{mb}\left[\hat{C}_{01}+\hat{C}_{51}\varphi\sin\chi\varphi+\left(\hat{C}_{52}\varphi\sin\chi\varphi+\hat{C}_{62}\varphi\cos\chi\varphi\right)\frac{\mathcal{P}}{\vartheta}\right], \qquad \text{(A.33a)}
\end{aligned}
$$

where

$$
\hat{C}_{01}=-\frac{m}{\chi^4}\,,\qquad \hat{C}_{51}=-\frac{A_{31}m}{2\chi^3}\,,\qquad \hat{C}_{52}=-\frac{A_{32}m}{2\chi^3}\,,\qquad \hat{C}_{62}=\frac{A_{42}m}{2\chi^3}\,. \qquad \text{(A.33b)}
$$

Making use of the constants $\hat{C}_{01},\dots,\hat{C}_{62}$ solution

$$
W_{ob}=C_1\cos\varphi+C_2H\sin\varphi+C_3H\sin\chi\varphi+C_4\cos\chi\varphi-\varepsilon_{mb}\frac{m}{2\chi^3}\left(\frac{2}{\chi}+A_3\varphi\sin\chi\varphi-A_4H\varphi\cos\chi\varphi\right)
$$

can be manipulated into a more favorable form as

$$
\begin{aligned}
W_{ob}=\varepsilon_{mb}\Big[\hat{C}_{01}+\hat{C}_{11}\cos\varphi+\hat{C}_{41}\cos\chi\varphi+\hat{C}_{51}\varphi\sin\chi\varphi+ \\
+\left(\hat{C}_{12}\cos\varphi+\hat{C}_{22}H\sin\varphi+\hat{C}_{32}H\sin\chi\varphi+\hat{C}_{42}\cos\chi\varphi+\hat{C}_{52}\varphi\sin\chi\varphi+\hat{C}_{62}H\varphi\cos\chi\varphi\right)\frac{\mathcal{P}}{\vartheta}\Big]\,. \qquad \text{(A.34)}
\end{aligned}
$$

As regards the expression for the rotation we need the derivative of the former relation, therefore

$$
\begin{aligned}
-\psi_{o\eta b}\simeq W_{ob}^{(1)}=\varepsilon_{mb}\Big[-\hat{C}_{11}\sin\varphi+\left(\hat{C}_{51}-\hat{C}_{41}\chi\right)\sin\chi\varphi+\hat{C}_{51}\chi\varphi\cos\chi\varphi+\left(-\hat{C}_{12}\sin\varphi+\hat{C}_{22}H\cos\varphi+\right. \\
\left.+\left(\hat{C}_{32}\chi+\hat{C}_{62}\right)H\cos\chi\varphi+\left(\hat{C}_{52}-\hat{C}_{42}\chi\right)\sin\chi\varphi+\ \hat{C}_{52}\chi\varphi\cos\chi\varphi-\hat{C}_{62}H\chi\varphi\sin\chi\varphi\right)\frac{\mathcal{P}}{\vartheta}\Big]
\end{aligned}
$$

or what is the same

$$
\begin{aligned}
-\psi_{o\eta b}\simeq W_{ob}^{(1)}=\varepsilon_{mb}\left[K_{11}\sin\varphi+K_{41}\sin\chi\varphi+K_{51}\varphi\cos\chi\varphi+\right. \\
\left.+\left(K_{12}\sin\varphi+K_{22}\cos\varphi+K_{32}\cos\chi\varphi+K_{42}\sin\chi\varphi+\ K_{52}\varphi\cos\chi\varphi+K_{62}\varphi\sin\chi\varphi\right)\frac{\mathcal{P}}{\vartheta}\right]\,. \qquad \text{(A.35)}
\end{aligned}
$$

A.1.8 The Averaged Strain Increment

As already mentioned in Subsubsection 5.2.3 it is possible to obtain closed form solutions to the integrals (constants) I_{01}, I_{02}, I_{11}, I_{12}, I_{13} in (61). Here we shall present the value of some. Recalling the formula for the averaged axial strain we have two terms to deal with

$$
\frac{1}{\vartheta}\int_0^{\vartheta}W_{ob}\mathrm{d}\varphi=\varepsilon_{mb}\left[I_{02}\frac{\mathcal{P}}{\vartheta}+I_{01}\right]\ ; \qquad \text{(A.36a)}
$$

$$
\frac{1}{\vartheta}\int_0^{\vartheta}W_{ob}^{(1)}W_{o}^{(1)}\mathrm{d}\varphi=\varepsilon_{mb}\left[I_{13}\left(\frac{\mathcal{P}}{\vartheta}\right)^2+\frac{\mathcal{P}}{\vartheta}I_{12}+I_{11}\right]\,. \qquad \text{(A.36b)}
$$

Starting with the first one let us integrate that part of the displacement increment, which does not contain the loading $\mathcal{P}$. Therefore it follows that

$$
\begin{aligned}
I_{01}=\frac{1}{\vartheta}\int_0^{\vartheta}\left(\hat{C}_{01}+\hat{C}_{11}\cos\varphi+\hat{C}_{41}\cos\chi\varphi+\hat{C}_{51}\varphi\sin\chi\varphi\right)\mathrm{d}\varphi= \\
=\frac{1}{\chi^2\vartheta}\left[\chi^2\left(\hat{C}_{01}\vartheta+\hat{C}_{11}\sin\vartheta\right)+\hat{C}_{41}\chi\sin\chi\vartheta+\hat{C}_{51}\left(\sin\chi\vartheta-\chi\vartheta\cos\chi\vartheta\right)\right]\,. \qquad \text{(A.37a)}
\end{aligned}
$$

Integrating the remainder of the displacement increment yields

$$
\begin{aligned}
I_{02}=\frac{1}{\vartheta}\int_0^{\vartheta}\left(\hat{C}_{12}\cos\varphi+\hat{C}_{22}\sin\varphi+\hat{C}_{32}\sin\chi\varphi+\hat{C}_{42}\cos\chi\varphi+\hat{C}_{52}\varphi\sin\chi\varphi+\hat{C}_{62}\varphi\cos\chi\varphi\right)\mathrm{d}\varphi= \\
=\frac{1}{\chi^2\vartheta}\left[\chi^2\left(\hat{C}_{12}\sin\vartheta+(1-\cos\vartheta)\,\hat{C}_{22}\right)+\hat{C}_{52}\sin\chi\vartheta+(\cos\chi\vartheta-1)\,\hat{C}_{62}+\right.
\end{aligned}
$$

$$+\chi\left(\left(1-\cos\chi\vartheta\right)\hat{C}_{32}+\hat{C}_{42}\sin\chi\vartheta-\hat{C}_{52}\vartheta\cos\chi\vartheta+\hat{C}_{62}\vartheta\sin\chi\vartheta\right)\Big]\ . \quad \text{(A.37b)}$$

Observe that I_{01} and I_{02} are the only integrals (constants) that appear in the part of the axial strain increment, which is obtained by neglecting the effect of the square of the rotation field – the corresponding equation

$$I_{02}\frac{\mathcal{P}}{\vartheta}+I_{01}=1 \quad \text{(A.38)}$$

is linear in $\mathcal{P}$.

As for the second integral in (A.36) let us recall formulae (58) and (59) providing the rotations and then separate the terms depending on the power of $(\mathcal{P}/\vartheta)$. Consequently

$$\begin{aligned}
\frac{1}{\vartheta}\int_0^{\vartheta}\psi_{o\eta}\psi_{o\eta\,b}\mathrm{d}\varphi &\approx \frac{1}{\vartheta}\int_0^{\vartheta}\left(-W_o^{(1)}\right)\left(-W_{ob}^{(1)}\right)\mathrm{d}\varphi= \\
&=-\varepsilon_{mb}\frac{1}{\vartheta}\int_0^{\vartheta}\Big[\left(K_{11}\sin\varphi+K_{41}\sin\chi\varphi+K_{51}\,\varphi\cos\chi\varphi\right)+ \\
&\quad+\frac{\mathcal{P}}{\vartheta}\left(K_{12}\sin\varphi+K_{22}\cos\varphi+K_{32}\cos\chi\varphi+K_{42}\sin\chi\varphi+K_{52}\varphi\cos\chi\varphi+K_{62}\varphi\sin\chi\varphi\right)\Big]\times \\
&\quad\times\left[D_{11}\sin\varphi+D_{31}\sin\chi\varphi+\left(D_{12}\sin\varphi+D_{22}\cos\varphi+D_{32}\sin\chi\varphi+D_{42}\cos\chi\varphi\right)\frac{\mathcal{P}}{\vartheta}\right]\mathrm{d}\varphi= \\
&\quad=-\varepsilon_{mb}\frac{1}{\vartheta}\int_0^{\vartheta}\left[\left(K_{11}\sin\varphi+K_{41}\sin\chi\varphi+K_{51}\,\varphi\cos\chi\varphi\right)\left(D_{11}\sin\varphi+D_{31}\sin\chi\varphi\right)+\right. \\
&\quad+\left(K_{11}\sin\varphi+K_{41}\sin\chi\varphi+K_{51}\,\varphi\cos\chi\varphi\right)\left(D_{12}\sin\varphi+D_{22}\cos\varphi+D_{32}\sin\chi\varphi+D_{42}\cos\chi\varphi\right)\frac{\mathcal{P}}{\vartheta}+ \\
&\quad+\left(K_{12}\sin\varphi+K_{22}\cos\varphi+K_{32}\cos\chi\varphi+K_{42}\sin\chi\varphi+K_{52}\varphi\cos\chi\varphi+K_{62}\varphi\sin\chi\varphi\right)\left(D_{11}\sin\varphi+D_{31}\sin\chi\varphi\right)\frac{\mathcal{P}}{\vartheta}+ \\
&\quad+\left(K_{12}\sin\varphi+K_{22}\cos\varphi+K_{32}\cos\chi\varphi+K_{42}\sin\chi\varphi+K_{52}\varphi\cos\chi\varphi+K_{62}\varphi\sin\chi\varphi\right)\times \\
&\quad\left.\times\left(D_{12}\sin\varphi+D_{22}\cos\varphi+D_{32}\sin\chi\varphi+D_{42}\cos\chi\varphi\right)\left(\frac{\mathcal{P}}{\vartheta}\right)^2\right]\mathrm{d}\varphi
\end{aligned}$$

in which

$$I_{11}=-\frac{1}{\vartheta}\int_0^{\vartheta}\left(K_{11}\sin\varphi+K_{41}\sin\chi\varphi+K_{51}\,\varphi\cos\chi\varphi\right)\left(D_{11}\sin\varphi+D_{31}\sin\chi\varphi\right)\mathrm{d}\varphi\ , \quad \text{(A.39a)}$$

$$\begin{aligned}
I_{12}=&-\frac{1}{\vartheta}\int_0^{\vartheta}\left(D_{11}\sin\varphi+D_{31}\sin\chi\varphi\right)\times \\
&\times\left(K_{12}\sin\varphi+K_{22}\cos\varphi+K_{32}\cos\chi\varphi+K_{42}\sin\chi\varphi+K_{52}\varphi\cos\chi\varphi+K_{62}\varphi\sin\chi\varphi\right)\mathrm{d}\varphi- \\
&-\frac{1}{\vartheta}\int_0^{\vartheta}\left(K_{11}\sin\varphi+K_{41}\sin\chi\varphi+K_{51}\,\varphi\cos\chi\varphi\right)\left(D_{12}\sin\varphi+D_{22}\cos\varphi+D_{32}\sin\chi\varphi+D_{42}\cos\chi\varphi\right)\mathrm{d}\varphi\,,
\end{aligned} \quad \text{(A.39b)}$$

$$\begin{aligned}
I_{13}=&-\frac{1}{\vartheta}\int_0^{\vartheta}\left(D_{12}\sin\varphi+D_{22}\cos\varphi+D_{32}\sin\chi\varphi+D_{42}\cos\chi\varphi\right)\times \\
&\times\left(K_{12}\sin\varphi+K_{22}\cos\varphi+K_{32}\cos\chi\varphi+K_{42}\sin\chi\varphi+K_{52}\varphi\cos\chi\varphi+K_{62}\varphi\sin\chi\varphi\right)\mathrm{d}\varphi\ .
\end{aligned} \quad \text{(A.39c)}$$

It can now be accepted that it is in fact possible to obtain closed form solutions. We omit them from being presented here as these are very complex and would require a lot of space. Mathematical softwares like Maple 16 or Scientific Work Place 5.5 can cope with these constants easily. Our aim is just to demonstrate the possibility of such solutions.

References

Baksa, A.; Ecsedi, I.: A note on the pure bending of nonhomogenous prismatic bars. *International Journal of Mechanical Engineering Education*, 37, 2, (2009), 118–129.

Bateni, M.; Eslami, M. R.: Non-linear in-plane stability analysis of FGM circular shallow arches under central concentrated force. *International Journal of Non-Linear Mechanics*, 60, (2014), 58–69.

Bradford, M. A.; Uy, B.; Pi, Y. L.: In-plane elastic stability of arches under a central concentrated load. *Journal of Engineering Mechanics*, 128, 7, (2002), 710–719.

Bresse, J. A. C.: *Recherches analytiques sur la flexion et la résistance des piéces courbes*. Mallet-Bachelier and Carilian-Goeury at V^r Dalmont, Paris (1854).

Burmeister, D.: Stability of shell-stiffened and axisymmetrically loaded annular plates. *Technische Mechanik*, 33, 1, (2013), 1–18.

Calboun, P. R.; DaDeppo, D. A.: Nonlinear finite element analysis of clamped arches. *Journal of Structural Engineering, ASCE*, 109, 3, (1983), 599–612.

Chen, Y.; Feng, J.: Elastic stability of shallow pin-ended parabolic arches subjected to step loads. *Journal of Central South University of Technology*, 17, (2010), 156–162.

Chidamparam, P.; Leissa, A. W.: Vibrations of planar curved beams, rings and arches. *Applied Mechanis Review, ASME*, 46, 9, (1993), 467–483.

Chwalla, E.; Kollbrunner, C. F.: Beiträge zum Knickproblem des Bogenträgers und des Rahmens. *Stahlbau*, 11, 10, (1938), 73–78.

DaDeppo, D. A.; Schmidt, R.: Sidesway buckling of deep crcular arches under a concentrated load. *Journal of Applied Mechanics,ASME*, 36, 6, (1969), 325–327.

DaDeppo, D. A.; Schmidt, R.: Large deflections and stability of hingeless circular arches under interacting loads. *Journal of Applied Mechanics, ASME*, 41, 4, (1974), 989–994.

Dym, C. L.: Bifurcation analyses for shallow arches. *Journal of the Engineering Mechanics Division, ASCE*, 99, EM2, (1973a), 287.

Dym, C. L.: Buckling and postbuckling behaviour of steep compressible arches. *International Journal of Solids and Structures*, 9, 1, (1973b), 129.

Dym, C. L.: *Stability Theory and Its Applications to Structural Mechanics*. Dover (1974, 2002).

Ecsedi, I.; Dluhi, K.: A linear model for the static and dynamic analysis of non-homogeneous curved beams. *Applied Mathematical Modelling*, 29, 12, (2005), 1211–1231.

Elias, Z. M.; Chen, K. L.: Nonlinear shallow curved beam finite element. *Journal of Engineering Mechanics, ASCE*, 114, 6, (1988), 1076–1087.

Huang, C. S.; Nieh, K. Y.; Yang, M. C.: In plane free vibration and stability of loaded and shear-deformable circular arches. *International Journal of Solids and Structures*, 40, (2003), 5865–5886.

Hurlbrink, E.: Festigkeitsberechnung von röhrenartigen Körpern, die unter äusserem Druck stehen. *Schiffbau*, 9, 14, (1907-1908), 517–523.

Kiss, L.: A possible model for heterogeneous curved beams. *Multidiszciplináris tudományok*, 2, 1, (2012), 61–76 (in Hungarian).

Laura, P. A. A.; Maurizi, M. J.: Recent research on vibrations of arch-type structures. *The Shock and Vibration Digest*, 19, 1, (1987), 6–9.

Love, A. E. H.: *A treatise on the mathematical theory of elasticity I. and II.*. Cambridge: University Press (1892 and 1893).

Love, A. E. H.: *A treatise on the mathematical theory of elasticity*. Cambridge: University Press, Second edn. (1906).

Márkus, S.; Nánási, T.: Vibration of curved beams. *The Shock and Vibration Digest*, 13, 4, (1981), 3–14.

Nieh, K. Y.; Huang, C. S.; Yang, M. C.: An analytical solution for in-plane free vibration and stability of loaded elliptic arches. *Computers and Structures*, 81, (2003), 1311–1327.

Noor, A. K.; Peters, J. M.: Mixed model and reduced/selective integration displacment modells for nonlinear analysis of curved beams. *International Journal of Numerical Methods in Engineering*, 17, 4, (1981), 615–631.

Pi, Y. L.; Bradford, M. A.: Dynamic buckling of shallow pin-ended arches under a sudden central concentrated load. *Journal of Sound and Vibration*, 317, (2008), 898–917.

Pi, Y.-L.; Bradford, M. A.: Non-linear buckling and postbuckling analysis of arches with unequal rotational end restraints under a central concentrated load. *International Journal of Solids and Structures*, 49, (2012), 3762–3773.

Pi, Y. L.; Bradford, M. A.; Tin-Loi, F.: Non-linear in-plane buckling of rotationally restrained shallow arches under a central concentrated load. *International Journal of Non-Linear Mechanics*, 43, (2008), 1–17.

Pi, Y. L.; Trahair, N. S.: Non-linear buckling and postbuckling of elastic arches. *Engineering Structures*, 20, 7, (1998), 571–579.

R. A. M. Silveira, C. L. N.; Goncalves, P. B.: A numerical approach for equilibrium and stability analysis of slender arches and rings under contact constraints. *International Journal of Solids and Structures*, 50, (2013), 147–159.

Schreyer, H. L.; Masur, E. F.: Buckling of shallow arches. *Journal of Engineering Mechanics Divison, ASCE*, 92, EM4, (1965), 1–19.

Szabó, B.; Királyfalvi, G.: Linear models of buckling and stress stiffening. *Computer Methods in Applied Mechanics*, 171, 1-2, (1999), 43–59.

Szeidl, G.: *Effect of Change in Length on the Natural Frequencies and Stability of Circular Beams*. Ph.D Thesis, Department of Mechanics, University of Miskolc, Hungary (1975), (in Hungarian).

Timoshenko, S. P.; Gere, J. M.: *Theory of Elastic Stability*. Engineering Sociaties Monograps, McGraw-Hill, 2^{nd} edn. (1961).

Wen, R. K.; Suhendro, B.: Nonlinear curved beam element for arch structures. *Journal of Structural Engineering, ASCE*, 117, 11, (1991), 3496–3515.

Address: Institute of Applied Mechanics, University of Miskolc, 3515 Miskolc-Egyetemváros, Hungary
email: mechkiss@uni-miskolc.hu, gyorgy.szeidl@uni-miskolc.hu